STATISTICS, OPTIMIZATION AND INFORMATION COMPUTING
Stat., Optim. Inf. Comput., Vol. **xx**, Month 2026, pp 0–35.
Published online in International Academic Press (www.IAPress.org)

Theory-Driven Inference and Data Modeling for the Odd Weibull-G Negative Binomial Class

Mahmoud El-Morshedy [1], Ibrahim Elbatal [2], M. H. Harpy [1], Mohamed S. Eliwa [3,4,*]

[1]*Department of Mathematics, College of Science and Humanities in Al-Kharj, Prince Sattam bin Abdulaziz University, Al-Kharj 11942, Saudi Arabia*
[2]*Department of Mathematics and Statistics, Faculty of Science, Imam Mohammad Ibn Saud Islamic University (IMSIU), Riyadh 11432, Saudi Arabia*
[3]*Department of Statistics and Operations Research, College of Science, Qassim University, Saudi Arabia*
[4]*Department of Mathematics, Faculty of Science, Mansoura University, Mansoura 35516, Egypt*

Abstract The need for flexible lifetime models that accommodate non-monotone hazard shapes has driven the development of numerous generators that extend classical baseline distributions. This paper introduces the odd Weibull–G negative binomial (WG–NB) family, a new class of distributions constructed by compounding the odd Weibull–G generator with a negative binomial scheme. The proposed family is motivated by the limitation of existing generators in capturing bathtub, unimodal, and reversed-J-shaped hazard rates while retaining a tractable analytical structure. Several structural and mathematical properties are derived, including a useful series expansion of the density function, ordinary and incomplete moments, moment generating function, mean deviations, Lorenz and Bonferroni curves, moments of residual and reversed residual life, and Shannon and Rényi entropies. A characterization based on two truncated moments is also established. For estimation, the maximum likelihood approach is developed, along with the maximum product spacing and Bayesian approaches. A simulation study examines the performance of the proposed estimators, and the flexibility of the new family is illustrated through the analysis of two real datasets using the AIC, CAIC, HQIC, the Kolmogorov-Smirnov statistic with its P-value, and the Anderson-Darling and Cramér–von Mises statistics. The results show that the WG–NB family provides a better fit than several competing models and offers a practical alternative for modelling lifetime and reliability data.

Keywords statistical model; hazard rate function; moments; residual life; entropy; maximum likelihood estimation; Bayesian estimation; characterization; simulation; lifetime data.

MSC2020: 60E05; 62E15; 62F10; 62N05; 62F15.

DOI: 10.19139/soic-2310-5070-4736

1. Introduction

In an era of increasing data-driven decision making, the data collected by researchers in medical science, bioengineering, environmental studies, actuarial science, economics and reliability engineering are often noisy, heterogeneous and inherently uncertain. Observations on lifetime and survival, whether they originate from clinical follow-up of disease evolution, fatigue tests on aeronautical materials or degradation monitoring of industrial systems, hardly satisfy the idealised assumptions of classical statistical models. The problem is aggravated by incomplete results due to short follow-up periods, patient dropout or pre-specified ending rules. Such practical limits urge the employment of current censoring systems such as hybrid and adaptive progressive censoring schemes. Probability distributions give a coherent mathematical framework for assessing uncertainty and allowing reliable inference about essential properties such as skewness, tail behaviour and failure risk. Classical distributions,

*Correspondence to: Mohamed S. Eliwa (Email: m.eliwa@qu.edu.sa ; mseliwa@mans.edu.eg)

ISSN 2310-5070 (online) ISSN 2311-004X (print)
Copyright © 2026 International Academic Press

however elegant and historically successful, are often too rigid for modern applications. Real survival and reliability data often exhibit large tails, strong asymmetry, and complex hazard-rate dynamics (including increasing, decreasing, unimodal, J-shaped, inverse-J-shaped, and bathtub-shaped patterns). As a single classical model cannot account for such variability, enforcing a poorly fitting distribution can result in skewed risk estimates, misleading reliability projections and ultimately inaccurate scientific results.

These restrictions have motivated a vibrant and continuing research program to build adaptable families of distributions by augmenting well-known basic models with new shape parameters, compounding schemes, or functional transformations. The aim is to increase the flexibility of the models while keeping analytical tractability and enhancing the estimation and prediction performance. Among the early works are the beta-generated family [16], the gamma-generated family [34], the Marshall–Olkin extended family [20] and the general class proposed by [9]. In the expanded Marshall–Olkin framework, the Marshall–Olkin Type II exponentiated half logistic Gompertz-G family was recently constructed [21] and exhibits better flexibility for complex survival and dependability data. A related direction of progress has been the incorporation of trigonometric mechanisms into the classical generators. For instance, [25] introduced the Marshall–Olkin cosine Topp–Leone distribution family that provides further flexibility for complex survival patterns. Further developments of the landscape include new distributions such as the Weibull-power Cauchy distribution [30], the transmuted odd Fréchet-G family [4] and other structures thoroughly covered in [1]. Further, different flexible univariate and discrete generators have been introduced to accommodate skewed, over-dispersed, and zero-inflated data under different hazard structures [11, 13, 14]. These have recently been extended to bivariate settings to model dependence structures and joint asymmetry in interdisciplinary applications [12, 15].

Among these generalized constructs, one of the most influential and extensively used generators is the odd Weibull-G (W-G) family introduced by [6]. The W-G family embeds an arbitrary baseline distribution G into a Weibull structure to give a unifying mechanism to generate models with highly adaptable hazard-rate shapes. Extensive odd Weibull-type models have been developed in the literature, including the power-transformed generators [3, 10], the trigonometric extension for censored survival data [29] and the unit-interval models for proportional responses on $(0,1)$ [2, 22] based on this work. At the same time, sophisticated inferential frameworks, e.g., Bayesian MCMC methods in complex censoring schemes, have been proposed to increase the accuracy and reliability of estimations [31, 32]. But despite these gains, an essential gap remains. Many recent extensions obtain flexibility at the expense of large parametric complexity, which may lead to overfitting, identifiability problems, and computational instability; other models are not flexible enough to accommodate the entire spectrum of hazard-rate shapes encountered in practice. This calls for an urgent need for distribution families that provide an effective trade-off between parsimony and flexibility: models that can represent symmetric and strongly skewed data, that can capture non-monotone failure mechanisms (including unimodal and bathtub-shaped hazards) and that can remain computationally tractable under realistic censoring scenarios. This study fills this gap by providing a new extension of the W-G family that is parsimonious and highly flexible. The proposed family is capable of dealing with a broad range of hazard-rate shapes including monotone, unimodal, J-shaped, inverse-J-shaped, and bathtub-shaped profiles without loss of mathematical tractability. We define its structural and reliability properties, develop classical and Bayesian estimation algorithms under complete and censored sampling schemes, and analyze the performance through extensive Monte Carlo experiments and actual data applications. The model developed provides a powerful and flexible tool for survival analysis and reliability modelling for practitioners in health, biology and engineering. For $y \in D \subseteq \mathbb{R}$, and $\beta > 0$, the cumulative distribution function (CDF) and probability density function (PDF) of the W-G family proposed by [6] are given by

$$P(y;\beta,\boldsymbol{\varphi}) = \int_0^{\frac{G(y;\boldsymbol{\varphi})}{1-G(y;\boldsymbol{\varphi})}} \beta t^{\beta-1} e^{-t^{\beta}} dt = 1 - e^{-\left(\frac{G(y;\boldsymbol{\varphi})}{\overline{G}(y;\boldsymbol{\varphi})}\right)^{\beta}}, \tag{1.1}$$

and

$$p(y;\beta,\boldsymbol{\varphi}) = \beta g(y;\boldsymbol{\varphi}) \frac{G(y;\boldsymbol{\varphi})^{\beta-1}}{\overline{G}(y;\boldsymbol{\varphi})^{\beta+1}} e^{-\left(\frac{G(y;\boldsymbol{\varphi})}{\overline{G}(y;\boldsymbol{\varphi})}\right)^{\beta}}, \tag{1.2}$$

respectively, where $g(y;\boldsymbol{\varphi})$, $G(y;\boldsymbol{\varphi})$, and $\overline{G}(y;\boldsymbol{\varphi})$ are the PDF, CDF, and reliability function of any baseline distribution based on a vector of parameters $\boldsymbol{\varphi}$. Investigation of new distribution models is an important topic in recent research, allowing more flexibility for effective modelling of complicated data structures.

Notably, the negative binomial distribution has been extensively used in mixing methods of distributions and compounded with other distributions to build flexible models. For example, [19] used the exponential-negative binomial distribution to fit the system failure times, whereas [24] proposed a regression model to predict the cure of prostate cancer based on the negative binomial-beta Weibull distribution. Other contributions include the study of the Weibull negative binomial distribution by [28], the negative binomial-Lindley distribution proposed by [33], and the Burr XII negative binomial distribution studied by [27]. Researchers in [26] suggested a fresh strategy and developed a new family of univariate distributions by combining the negative binomial distribution with any continuous model. They introduced a general class of continuous distributions called the G-negative binomial (G-NB) class. For a positive random variable Z and any baseline CDF $H(z;\boldsymbol{\varphi})$, the CDF and PDF for the G-NB class are given by

$$V(z;\alpha,\theta,\boldsymbol{\varphi}) = \frac{(1-\alpha)^{-\theta} - [1-\alpha(1-H(z;\boldsymbol{\varphi}))]^{-\theta}}{[(1-\alpha)^{-\theta}-1]}, \tag{1.3}$$

and

$$v(z;\alpha,\theta,\boldsymbol{\varphi}) = \frac{\alpha\theta h(z;\boldsymbol{\varphi})\,[1-\alpha(1-H(z;\boldsymbol{\varphi}))]^{-(\theta+1)}}{[(1-\alpha)^{-\theta}-1]}, \tag{1.4}$$

respectively. The G-NB family includes the identical parameters of the $H(z;\boldsymbol{\varphi})$ distribution plus two additional shape parameters $\theta > 0$ and $\alpha \in (0,1)$. The aim of this study is to introduce a flexible family of distributions by integrating W-G and G-NB families. Substituting (1.1) into (1.3), we propose a new class of generators called the Weibull-G-negative binomial (WG-NB) class of distributions. For a positive random variable X, the CDF of the WG-NB family is given by

$$F(x;\alpha,\theta,\beta,\boldsymbol{\varphi}) = \frac{1}{[(1-\alpha)^{-\theta}-1]}\left\{(1-\alpha)^{-\theta} - \left[1-\alpha e^{-\left(\frac{G(x;\boldsymbol{\varphi})}{\overline{G}(x;\boldsymbol{\varphi})}\right)^{\beta}}\right]^{-\theta}\right\}. \tag{1.5}$$

The corresponding PDF is

$$f\,(x;\alpha,\theta,\beta,\boldsymbol{\varphi}) = \frac{\alpha\theta\beta g(x;\boldsymbol{\varphi})}{[(1-\alpha)^{-\theta}-1]}\frac{G(x;\boldsymbol{\varphi})^{\beta-1}}{\overline{G}(x;\boldsymbol{\varphi})^{\beta+1}} e^{-\left(\frac{G(x;\boldsymbol{\varphi})}{\overline{G}(x;\boldsymbol{\varphi})}\right)^{\beta}}\left[1-\alpha e^{-\left(\frac{G(x;\boldsymbol{\varphi})}{\overline{G}(x;\boldsymbol{\varphi})}\right)^{\beta}}\right]^{-(\theta+1)}. \tag{1.6}$$

Here, $G(x;\boldsymbol{\varphi})$ is the baseline CDF. In our proposal, we define the WG-NB class that provides probability models with asymmetric or symmetric shapes, permits different forms of kurtosis, specifies special probability models with different risk/failure rate functions, provides models appropriate for the analysis of over- and under-dispersed data, develops models for the analysis of lifetime datasets, and consistently outperforms the models available in the current literature.

This paper proceeds as follows. In Section 2, we examine special and limiting cases of the WG-NB distribution family. Section 3 develops the theoretical distributional properties. Section 4 presents both frequentist and Bayesian inferential procedures, including asymptotic confidence intervals and Bayesian estimation with credible intervals. The performance of the proposed methods is evaluated through an extensive Monte Carlo simulation study in Section 5. Section 6 demonstrates the practical applicability of the WG-NB distribution via empirical analysis of two real datasets. The paper concludes in Section 7 with a summary of key contributions and suggestions for future work.

2. Certain Special Models within the WG-NB Class

2.1. Weibull Fréchet Negative Binomial (WFNB) Distribution

The Fréchet distribution is a popular choice for modelling extreme values in several domains, including hydrology, economics and environmental sciences. The CDF and PDF of WFNB distribution are

$$F(x) = \frac{1}{[(1-\alpha)^{-\theta}-1]}\left\{(1-\alpha)^{-\theta} - \left[1-\alpha e^{-\left(e^{(\frac{a}{x})^b}-1\right)^{-\beta}}\right]^{-\theta}\right\},$$

and

$$f\,(x) = \frac{\alpha\theta\beta b a^b x^{-b-1} e^{-(\frac{a}{x})^b}}{[(1-\alpha)^{-\theta}-1]} \frac{(e^{-(\frac{a}{x})^b})^{\beta-1}}{(1-e^{-(\frac{a}{x})^b})^{\beta+1}} e^{-\left(e^{(\frac{a}{x})^b}-1\right)^{-\beta}} \left[1-\alpha e^{-\left(e^{(\frac{a}{x})^b}-1\right)^{-\beta}}\right]^{-(\theta+1)}.$$

Figure 1 shows that the WFNB density and hazard shapes are appropriate probabilistic tools for analyzing the symmetric and asymmetric data. Moreover, the WFNB HRF form can be seen in various patterns, such as declining, increasing, J-shaped, bathtub-shaped, and unimodal.

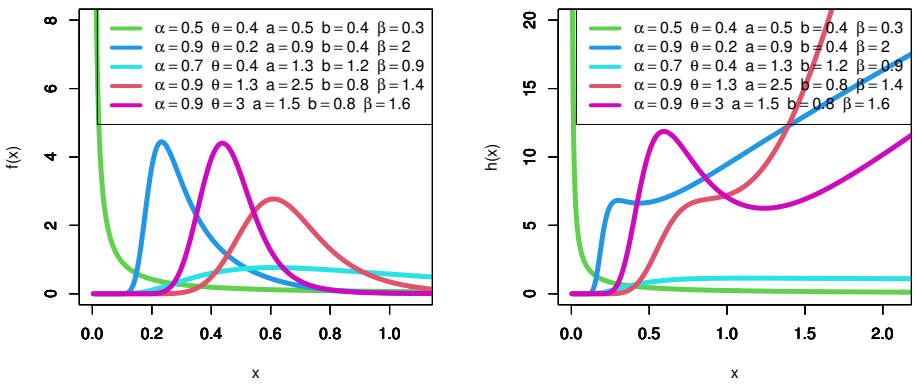


Figure 1. Density and hazard rate functions of the WFNB distribution.

2.2. Weibull Exponential Negative Binomial (WENB) Distribution

The exponential distribution is the distribution of probabilities for the duration between events in a Poisson process, where events occur continuously and independently at a constant average rate. It is typically used to represent the time until some event occurs. The CDF and PDF of the WENB model are given by

$$F(x) = \frac{1}{[(1-\alpha)^{-\theta}-1]}\left\{(1-\alpha)^{-\theta} - \left[1-\alpha e^{-(e^{\mu x}-1)^{\beta}}\right]^{-\theta}\right\},$$

and

$$f\,(x) = \frac{\alpha\theta\beta\mu e^{-\mu x}}{[(1-\alpha)^{-\theta}-1]} \frac{(1-e^{-\mu x})^{\beta-1}}{(e^{-\mu x})^{\beta+1}} e^{-(e^{\mu x}-1)^{\beta}} \left[1-\alpha e^{-(e^{\mu x}-1)^{\beta}}\right]^{-(\theta+1)}.$$

It can be seen in Figure 2 that the density and hazard shapes of the WENB can be used as a probabilistic device in the processing of asymmetric data. Moreover, it is pointed out that the HRF shape of the WENB can be of several types, including declining, rising, J-shaped, bathtub-shaped, and unimodal.

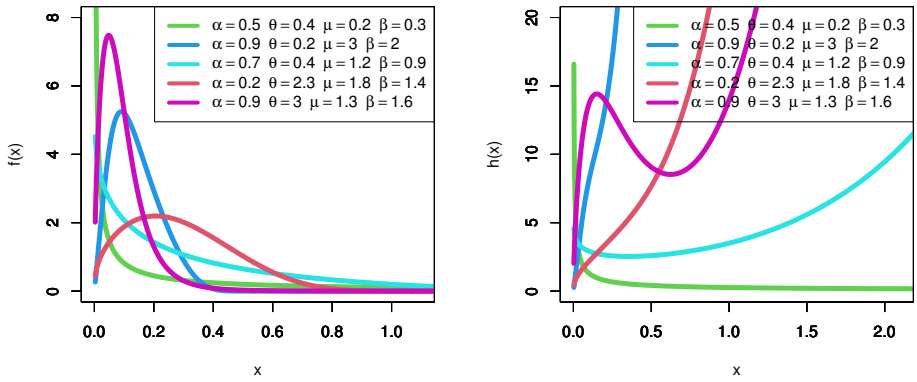


Figure 2. Density and hazard rate functions of the WENB distribution.

2.3. Weibull Rayleigh Negative Binomial (WRNB) Distribution

The Rayleigh distribution is a probability distribution used to simulate the distribution of the magnitude of a two-dimensional vector with independent, identically distributed Gaussian random variables as components. The CDF and PDF of the WRNB model can be formulated as

$$F(x) = \frac{1}{[(1-\alpha)^{-\theta}-1]}\left\{(1-\alpha)^{-\theta} - \left[1-\alpha e^{-\left(e^{\frac{\rho}{2}x^2}-1\right)^{\beta}}\right]^{-\theta}\right\},$$

and

$$f\,(x) = \frac{\alpha\theta\beta\rho x e^{-\frac{\rho}{2}x^2}}{[(1-\alpha)^{-\theta}-1]}\frac{(1-e^{-\frac{\rho}{2}x^2})^{\beta-1}}{(e^{-\frac{\rho}{2}x^2})^{\beta+1}} e^{-\left(e^{\frac{\rho}{2}x^2}-1\right)^{\beta}}\left[1-\alpha e^{-\left(e^{\frac{\rho}{2}x^2}-1\right)^{\beta}}\right]^{-(\theta+1)}.$$

Figure 3 indicates that the density and hazard shape of the WRNB are useful probabilistic tools for the analysis of asymmetric and symmetric data. Moreover, it is found that the HRF shape of the WRNB varies, which can be in the form of declining, increasing, J-shaped, bathtub-shaped and unimodal.

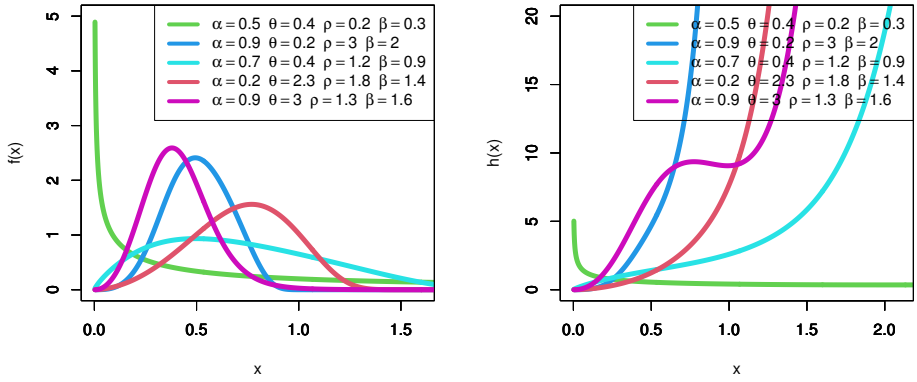


Figure 3. Density and hazard rate functions of the WRNB distribution.

3. Distributional Properties

This section investigates several mathematical properties of the WG–NB family. We first derive a useful series expansion of its density function and then examine moment-based measures, including ordinary and incomplete moments and related descriptive measures. We also obtain expressions for the moments of residual and reversed residual life and for Shannon and Rényi entropies. Finally, we present characterization results based on two truncated moments.

3.1. Useful Expansion of the WG–NB Density Function

Let

$$D = (1-\alpha)^{-\theta} - 1, \qquad z(x) = \left[\frac{G(x;\boldsymbol{\varphi})}{1-G(x;\boldsymbol{\varphi})}\right]^{\beta},$$

where $0 < \alpha < 1$, $\theta > 0$, and $\beta > 0$. The generalized binomial expansion

$$(1-u)^{-b} = \sum_{i=0}^{\infty} \frac{(b)_i}{i!} u^i, \qquad |u| < 1, \quad b > 0, \tag{3.1}$$

holds for every positive real b, including positive integers. Here, $(b)_i = \Gamma(b+i)/\Gamma(b)$ denotes the rising factorial, with $(b)_0 = 1$. Since $0 \le \alpha e^{-z(x)} < 1$, applying (3.1) to the density gives

$$f(x) = \frac{\theta}{D} \sum_{i=0}^{\infty} \frac{(\theta+1)_i \alpha^{i+1}}{i!} z'(x) e^{-(i+1)z(x)}, \tag{3.2}$$

where

$$z'(x) = \beta g(x;\boldsymbol{\varphi}) \frac{G(x;\boldsymbol{\varphi})^{\beta-1}}{[1-G(x;\boldsymbol{\varphi})]^{\beta+1}}. \tag{3.3}$$

For each integer $m \ge 1$, define

$$H_m(x) = 1 - e^{-mz(x)} \tag{3.4}$$

and

$$\begin{aligned} h_m(x) &= m z'(x) e^{-mz(x)} \\ &= m\beta g(x;\boldsymbol{\varphi}) \frac{G(x;\boldsymbol{\varphi})^{\beta-1}}{[1-G(x;\boldsymbol{\varphi})]^{\beta+1}} e^{-mz(x)}. \end{aligned} \tag{3.5}$$

For an absolutely continuous baseline distribution, these are a CDF and its corresponding density on the baseline support. Reindexing (3.2) yields

$$f(x) = \sum_{m=1}^{\infty} p_m h_m(x), \qquad p_m = \frac{(\theta)_m \alpha^m}{D\, m!}. \tag{3.6}$$

Indeed,

$$p_m > 0, \qquad \sum_{m=1}^{\infty} p_m = \frac{1}{D}\left[\sum_{m=0}^{\infty} \frac{(\theta)_m \alpha^m}{m!} - 1\right] = 1. \tag{3.7}$$

Thus, (3.6) is a genuine probability mixture. By Tonelli's theorem, the corresponding CDF and survival function satisfy

$$F(x) = \sum_{m=1}^{\infty} p_m H_m(x), \qquad S(x) = \sum_{m=1}^{\infty} p_m e^{-mz(x)}. \tag{3.8}$$

In particular,

$$\sum_{m=1}^{\infty} p_m e^{-mz(x)} = \frac{[1-\alpha e^{-z(x)}]^{-\theta} - 1}{D},$$

which agrees with the survival function obtained directly from the WG–NB CDF. Although the exponential factor in (3.2) can itself be expanded into a Taylor series, the resulting alternating multiple series cannot, in general, be rearranged or integrated term by term. In particular, signed coefficients in an expansion in exponentiated-G densities are not probability-mixture weights. The nonnegative representation (3.6) avoids these difficulties and provides a justified basis for deriving distributional properties.

3.2. Moment-Based Measures

Assume in this subsection that X is positive. Let Y_m have density h_m defined in (3.5). For every nonnegative measurable function ψ, the mixture representation and Tonelli's theorem imply

$$\mathbb{E}[\psi(X)] = \sum_{m=1}^{\infty} p_m \mathbb{E}[\psi(Y_m)], \tag{3.9}$$

where equality remains valid when either side is infinite. For $r > 0$, the rth ordinary moment is

$$\mu'_r = \mathbb{E}[X^r] = \sum_{m=1}^{\infty} p_m \mathbb{E}[Y_m^r], \tag{3.10}$$

provided that the sum is finite. Let $Q_G(u;\boldsymbol{\varphi})$ denote the baseline quantile function, and define

$$\xi(v) = Q_G\left(\frac{v^{1/\beta}}{1+v^{1/\beta}};\boldsymbol{\varphi}\right), \qquad v > 0. \tag{3.11}$$

Under the component distribution H_m, the transformed variable $z(Y_m)$ has an exponential distribution with rate m. Consequently,

$$\mathbb{E}[Y_m^r] = m\int_0^{\infty} \xi(v)^r e^{-mv}\,\mathrm{d}v, \tag{3.12}$$

and therefore

$$\mu'_r = \sum_{m=1}^{\infty} p_m m \int_0^{\infty} \xi(v)^r e^{-mv}\,\mathrm{d}v. \tag{3.13}$$

The existence of these moments depends on the baseline distribution and must be checked separately. For an integer $r \geq 1$ with $\mu'_r < \infty$, the rth central moment is

$$\mu_r = \mathbb{E}[(X-\mu'_1)^r] = \sum_{k=0}^{r} \binom{r}{k} (-\mu'_1)^{r-k}\mu'_k, \qquad \mu'_0 = 1. \tag{3.14}$$

In particular,

$$\begin{aligned} \mu_2 &= \mu'_2 - (\mu'_1)^2, \\ \mu_3 &= \mu'_3 - 3\mu'_1\mu'_2 + 2(\mu'_1)^3, \\ \mu_4 &= \mu'_4 - 4\mu'_1\mu'_3 + 6(\mu'_1)^2\mu'_2 - 3(\mu'_1)^4. \end{aligned} \tag{3.15}$$

When the relevant moments are finite and $\mu_2 > 0$, skewness and kurtosis are

$$\gamma_1 = \frac{\mu_3}{\mu_2^{3/2}}, \qquad \gamma_2 = \frac{\mu_4}{\mu_2^2}, \tag{3.16}$$

respectively. Excess kurtosis is $\gamma_2 - 3$. For every real s at which the expectation is finite,

$$\begin{aligned} M_X(s) &= \mathbb{E}[e^{sX}] \\ &= \sum_{m=1}^{\infty} p_m M_{Y_m}(s) \\ &= \sum_{m=1}^{\infty} p_m m \int_0^{\infty} \exp\{s\xi(v) - mv\}\,\mathrm{d}v. \end{aligned} \tag{3.17}$$

Because the integrands are nonnegative, the mixture identity also holds in the extended sense when the expectation is infinite. For positive X, $M_X(s)$ is finite for every $s \leq 0$. However, existence on an open neighborhood of zero requires finiteness for some $s > 0$ and is not guaranteed by the WG–NB construction. When such a neighborhood exists, the MGF uniquely determines the distribution. For $r \geq 0$ and $t > 0$, define the lower incomplete moment

$$\zeta_r(t) = \int_0^t x^r f(x)\,\mathrm{d}x. \tag{3.18}$$

The nonnegative mixture gives

$$\zeta_r(t) = \sum_{m=1}^{\infty} p_m \int_0^t x^r h_m(x)\,\mathrm{d}x. \tag{3.19}$$

Writing $z_t = z(t)$ and applying $v = z(x)$, we obtain

$$\zeta_r(t) = \sum_{m=1}^{\infty} p_m m \int_0^{z_t} \xi(v)^r e^{-mv}\,\mathrm{d}v. \tag{3.20}$$

In particular, $\zeta_0(t) = F(t)$. For $r > 0$, $0 \leq \zeta_r(t) \leq t^r F(t)$, so lower incomplete moments are finite even when the corresponding ordinary moments are infinite. Similarly, the upper incomplete moment is

$$\begin{aligned} \overline{\zeta}_r(t) &= \int_t^{\infty} x^r f(x)\,\mathrm{d}x \\ &= \sum_{m=1}^{\infty} p_m m \int_{z_t}^{\infty} \xi(v)^r e^{-mv}\,\mathrm{d}v. \end{aligned} \tag{3.21}$$

If $\mu'_r < \infty$, then $\overline{\zeta}_r(t) = \mu'_r - \zeta_r(t)$. For comparison, if Z_δ has an exponentiated-G density $\pi_\delta(x) = \delta g(x;\boldsymbol{\varphi})G(x;\boldsymbol{\varphi})^{\delta-1}$, its lower incomplete moment is

$$\int_0^t x^r \pi_\delta(x)\,\mathrm{d}x = \delta \int_0^{G(t;\boldsymbol{\varphi})} u^{\delta-1} Q_G(u;\boldsymbol{\varphi})^r\,\mathrm{d}u. \tag{3.22}$$

The exponent of u is $\delta - 1$, not δ. This identity does not, by itself, justify an exponentiated-G mixture representation for the WG–NB distribution. Assume that $\mu = \mu'_1 < \infty$. For any $a > 0$, splitting the expectation at a gives

$$\mathbb{E}[|X - a|] = \mu - a + 2aF(a) - 2\zeta_1(a). \tag{3.23}$$

Thus, the mean deviation about the mean is

$$\delta_\mu = 2\mu F(\mu) - 2\zeta_1(\mu). \tag{3.24}$$

If M is a median satisfying $F(M) = 1/2$, then the mean deviation about the median is

$$\delta_M = \mu - 2\zeta_1(M). \tag{3.25}$$

Suppose that $0 < \mu < \infty$, and let $Q(p)$ denote the WG–NB quantile function. Solving the CDF equation gives, for $0 < p < 1$,

$$\begin{aligned} B_p &= (1-\alpha)^{-\theta} - pD, \\ v_p &= -\log\left(\frac{1 - B_p^{-1/\theta}}{\alpha}\right), \\ Q(p) &= Q_G\left(\frac{v_p^{1/\beta}}{1 + v_p^{1/\beta}}; \boldsymbol{\varphi}\right). \end{aligned} \tag{3.26}$$

For a continuous, strictly increasing CDF, the Lorenz curve is

$$L(p) = \frac{1}{\mu}\int_0^p Q(u)\,\mathrm{d}u = \frac{\zeta_1(Q(p))}{\mu}, \qquad 0 < p < 1, \tag{3.27}$$

and the Bonferroni curve is

$$B(p) = \frac{L(p)}{p} = \frac{\zeta_1(Q(p))}{p\mu}, \qquad 0 < p < 1. \tag{3.28}$$

These curves are therefore computable from the first lower incomplete moment in (3.20).

3.3. Moments of Residual and Reversed Residual Life

Residual and reversed residual life describe, respectively, the remaining lifetime of a unit that has survived to a specified age and the elapsed time since failure of a unit known to have failed before that age. Let X be a positive random variable following the WG–NB distribution, with $0 < \alpha < 1$, $\theta > 0$, $\beta > 0$, and baseline parameter vector $\boldsymbol{\varphi}$. For notational simplicity, define

$$D = (1-\alpha)^{-\theta} - 1, \qquad z(x) = \left[\frac{G(x;\boldsymbol{\varphi})}{1-G(x;\boldsymbol{\varphi})}\right]^{\beta}, \qquad A(x) = \left[1 - \alpha e^{-z(x)}\right]^{-\theta}. \tag{3.29}$$

The distribution and survival functions can then be written as

$$F(x) = \frac{(1-\alpha)^{-\theta} - A(x)}{D}, \qquad S(x) = 1 - F(x) = \frac{A(x) - 1}{D}. \tag{3.30}$$

All expressions below are evaluated at ages $t > 0$ for which the relevant conditioning event has positive probability. The residual life at age t is the conditional random variable $R_t = (X - t) \mid X > t$. For a positive integer r, its rth raw moment is

$$m_r(t) = \mathbb{E}\left[(X-t)^r \mid X > t\right] = \frac{1}{S(t)}\int_t^{\infty} (x-t)^r f(x)\,\mathrm{d}x, \qquad S(t) > 0, \tag{3.31}$$

provided that the integral is finite. Its conditional survival function is

$$\Pr(R_t > y) = \frac{S(t+y)}{S(t)} = \frac{A(t+y) - 1}{A(t) - 1}, \qquad y \geq 0. \tag{3.32}$$

Using the tail-integral identity for nonnegative random variables gives

$$\begin{aligned} m_r(t) &= \frac{r}{S(t)}\int_t^{\infty} (x-t)^{r-1} S(x)\,\mathrm{d}x \\ &= \frac{r}{A(t)-1}\int_t^{\infty} (x-t)^{r-1}\left\{\left[1 - \alpha e^{-z(x)}\right]^{-\theta} - 1\right\}\mathrm{d}x. \end{aligned} \tag{3.33}$$

This identity also holds in the extended sense when the moment is infinite. An equivalent representation follows from upper incomplete moments. Define

$$M_k^{+}(t) = \int_t^{\infty} x^k f(x)\,\mathrm{d}x, \qquad k = 0, 1, \ldots, \tag{3.34}$$

so that $M_0^{+}(t) = S(t)$. If $M_r^{+}(t) < \infty$, the binomial expansion yields

$$m_r(t) = \frac{1}{S(t)}\sum_{k=0}^{r}\binom{r}{k}(-t)^{r-k} M_k^{+}(t). \tag{3.35}$$

In particular, the mean residual life is

$$\begin{aligned} m_1(t) &= \frac{1}{S(t)} \int_t^\infty S(x)\,\mathrm{d}x \\ &= \frac{\displaystyle\int_t^\infty [A(x)-1]\,\mathrm{d}x}{A(t)-1} = \frac{M_1^+(t)}{S(t)} - t. \end{aligned} \tag{3.36}$$

When the second moment is finite,

$$m_2(t) = \frac{2}{A(t)-1} \int_t^\infty (x-t)[A(x)-1]\,\mathrm{d}x, \qquad \mathrm{Var}(R_t) = m_2(t) - m_1(t)^2. \tag{3.37}$$

The reversed residual life at age t is the conditional random variable $B_t = (t-X) \mid X \le t$. Its rth raw moment is

$$b_r(t) = \mathbb{E}\left[(t-X)^r \mid X \le t\right] = \frac{1}{F(t)} \int_0^t (t-x)^r f(x)\,\mathrm{d}x, \qquad F(t) > 0. \tag{3.38}$$

Since $0 \le B_t \le t$, these moments are finite for every positive integer r. Absolute continuity gives

$$\Pr(B_t > y) = \frac{F(t-y)}{F(t)}, \qquad 0 \le y \le t. \tag{3.39}$$

Consequently,

$$\begin{aligned} b_r(t) &= \frac{r}{F(t)} \int_0^t (t-x)^{r-1} F(x)\,\mathrm{d}x \\ &= \frac{r}{(1-\alpha)^{-\theta} - A(t)} \int_0^t (t-x)^{r-1} \left\{ (1-\alpha)^{-\theta} - \left[1 - \alpha e^{-z(x)}\right]^{-\theta} \right\} \mathrm{d}x. \end{aligned} \tag{3.40}$$

Define the lower incomplete moments by

$$M_k^-(t) = \int_0^t x^k f(x)\,\mathrm{d}x, \qquad k = 0, 1, \ldots, \tag{3.41}$$

where $M_0^-(t) = F(t)$. Expanding $(t-x)^r$ gives

$$b_r(t) = \frac{1}{F(t)} \sum_{k=0}^{r} (-1)^k \binom{r}{k} t^{r-k} M_k^-(t). \tag{3.42}$$

Thus, the mean reversed residual life, also called the mean inactivity time, is

$$\begin{aligned} b_1(t) &= \frac{1}{F(t)} \int_0^t F(x)\,\mathrm{d}x \\ &= \frac{\displaystyle\int_0^t \left[(1-\alpha)^{-\theta} - A(x)\right]\,\mathrm{d}x}{(1-\alpha)^{-\theta} - A(t)} = t - \frac{M_1^-(t)}{F(t)}. \end{aligned} \tag{3.43}$$

The second raw moment and variance are

$$\begin{aligned} b_2(t) &= \frac{2}{(1-\alpha)^{-\theta} - A(t)} \int_0^t (t-x) \left[(1-\alpha)^{-\theta} - A(x)\right]\,\mathrm{d}x, \\ \mathrm{Var}(B_t) &= b_2(t) - b_1(t)^2. \end{aligned} \tag{3.44}$$

The incomplete moments can be evaluated using a transformation that separates the WG–NB parameters from the baseline quantile. Suppose that the baseline CDF is continuous and strictly increasing on its support, and let $Q_G(u;\boldsymbol{\varphi})$ denote its quantile function. Define

$$\xi(v) = Q_G\left(\frac{v^{1/\beta}}{1+v^{1/\beta}};\boldsymbol{\varphi}\right), \qquad v>0. \tag{3.45}$$

The substitution $v = z(x)$ satisfies

$$\mathrm{d}v = \beta g(x;\boldsymbol{\varphi})\frac{G(x;\boldsymbol{\varphi})^{\beta-1}}{[1-G(x;\boldsymbol{\varphi})]^{\beta+1}}\,\mathrm{d}x, \tag{3.46}$$

and hence

$$f(x)\,\mathrm{d}x = \frac{\alpha\theta}{D}e^{-v}\left(1-\alpha e^{-v}\right)^{-(\theta+1)}\,\mathrm{d}v. \tag{3.47}$$

Writing $z_t = z(t)$, the incomplete moments become

$$M_k^-(t) = \frac{\alpha\theta}{D}\int_0^{z_t}\xi(v)^k e^{-v}\left(1-\alpha e^{-v}\right)^{-(\theta+1)}\,\mathrm{d}v \tag{3.48}$$

and

$$M_k^+(t) = \frac{\alpha\theta}{D}\int_{z_t}^{\infty}\xi(v)^k e^{-v}\left(1-\alpha e^{-v}\right)^{-(\theta+1)}\,\mathrm{d}v. \tag{3.49}$$

For $k=0$, the factor $\xi(v)^k$ is understood to be one. These representations provide one-dimensional integral formulas for computing the residual and reversed residual life moments under a specified baseline distribution. The existence of upper incomplete moments, and therefore of residual life moments, depends on the upper-tail behavior of that baseline; it is not guaranteed by the WG–NB generator alone.

3.4. Entropy

Entropy measures the uncertainty associated with a probability distribution. For the WG–NB family, Shannon and Rényi entropies can be expressed in terms of one-dimensional integrals involving the baseline quantile function. Throughout this subsection, logarithms are natural, so that entropy is measured in nats. Assume that $0<\alpha<1$, $\theta>0$, and $\beta>0$, and that the baseline CDF is strictly increasing and continuously differentiable on its support, with positive density there. Define

$$D = (1-\alpha)^{-\theta}-1, \qquad C = \frac{\alpha\theta}{D}, \qquad z(x) = \left[\frac{G(x;\boldsymbol{\varphi})}{1-G(x;\boldsymbol{\varphi})}\right]^{\beta}. \tag{3.50}$$

The derivative of the transformation $z(x)$ is

$$z'(x) = \beta g(x;\boldsymbol{\varphi})\frac{G(x;\boldsymbol{\varphi})^{\beta-1}}{[1-G(x;\boldsymbol{\varphi})]^{\beta+1}}, \tag{3.51}$$

and the WG–NB density can therefore be written as

$$f(x) = Cz'(x)e^{-z(x)}\left[1-\alpha e^{-z(x)}\right]^{-(\theta+1)}. \tag{3.52}$$

Let $Q_G(u;\boldsymbol{\varphi})$ be the baseline quantile function, and define the inverse transformation

$$\xi(v) = Q_G\left(\frac{v^{1/\beta}}{1+v^{1/\beta}};\boldsymbol{\varphi}\right), \qquad v>0. \tag{3.53}$$

Its derivative is

$$w(v) = \xi'(v) = \frac{v^{1/\beta-1}}{\beta[1+v^{1/\beta}]^2 g(\xi(v);\boldsymbol{\varphi})}. \tag{3.54}$$

Consequently, the transformed variable $V = z(X)$ has density

$$p_V(v) = Ce^{-v}\left(1-\alpha e^{-v}\right)^{-(\theta+1)}, \qquad v > 0, \tag{3.55}$$

and

$$f(\xi(v)) = \frac{p_V(v)}{w(v)}. \tag{3.56}$$

These identities separate the contribution of the WG–NB generator from that of the baseline distribution. The differential Shannon entropy is

$$\mathcal{H}(X) = -\int f(x)\log f(x)\,\mathrm{d}x = -\mathbb{E}[\log f(X)], \tag{3.57}$$

where integration is over the support of X. A finite value requires $\mathbb{E}[|\log f(X)|] < \infty$. Using (3.56), we obtain

$$\mathcal{H}(X) = -\log C + \mathbb{E}[V] + (\theta+1)\mathbb{E}\left[\log(1-\alpha e^{-V})\right] + \mathbb{E}[\log w(V)]. \tag{3.58}$$

The expectations in this expression are taken with respect to (3.55). The logarithmic expectation involving the generator admits an explicit expression. Indeed, the variable $Q = 1-\alpha e^{-V}$ has density

$$p_Q(q) = \frac{\theta}{D}q^{-\theta-1}, \qquad 1-\alpha < q < 1. \tag{3.59}$$

Hence,

$$\begin{aligned}\mathbb{E}[\log Q] &= \frac{\theta}{D}\int_{1-\alpha}^{1} q^{-\theta-1}\log q\,\mathrm{d}q \\ &= \frac{1}{\theta} + \frac{(1-\alpha)^{-\theta}\log(1-\alpha)}{D}.\end{aligned} \tag{3.60}$$

Furthermore, the binomial-series expansion

$$(1-\alpha e^{-v})^{-(\theta+1)} = \sum_{j=0}^{\infty}\frac{(\theta+1)_j}{j!}\alpha^j e^{-jv}, \tag{3.61}$$

where $(a)_j = \Gamma(a+j)/\Gamma(a)$ and $(a)_0 = 1$, gives

$$\begin{aligned}\mathbb{E}[V] &= C\sum_{j=0}^{\infty}\frac{(\theta+1)_j\alpha^j}{j!}\int_0^{\infty} v e^{-(j+1)v}\,\mathrm{d}v \\ &= C\sum_{j=0}^{\infty}\frac{(\theta+1)_j\alpha^j}{j!(j+1)^2}.\end{aligned} \tag{3.62}$$

The interchange of integration and summation follows from Tonelli's theorem because all terms are nonnegative. The series is finite for $0 < \alpha < 1$. Substitution into (3.58) yields

$$\begin{aligned}\mathcal{H}(X) = \log\left(\frac{D}{\alpha\theta}\right) &+ C\sum_{j=0}^{\infty}\frac{(\theta+1)_j\alpha^j}{j!(j+1)^2} \\ &+ (\theta+1)\left[\frac{1}{\theta} + \frac{(1-\alpha)^{-\theta}\log(1-\alpha)}{D}\right] \\ &+ C\int_0^{\infty} e^{-v}(1-\alpha e^{-v})^{-(\theta+1)}\log w(v)\,\mathrm{d}v.\end{aligned} \tag{3.63}$$

This formula gives a finite entropy whenever the final integral is absolutely convergent. Alternatively, expanding $\log w(V)$ gives the baseline-explicit representation

$$\begin{aligned}\mathcal{H}(X) = \log\left(\frac{D}{\alpha\theta\beta}\right) &- \mathbb{E}[\log g(\xi(V);\boldsymbol{\varphi})] \\ &+ \left(\frac{1}{\beta}-1\right)\mathbb{E}[\log V] - 2\mathbb{E}\Big[\log(1+V^{1/\beta})\Big] + \mathbb{E}[V] \\ &+ (\theta+1)\left[\frac{1}{\theta} + \frac{(1-\alpha)^{-\theta}\log(1-\alpha)}{D}\right].\end{aligned} \tag{3.64}$$

Thus, although the distribution of V depends only on α and θ, the entropy of X also depends on β and the baseline distribution through the inverse transformation ξ. For an order $\rho > 0$, $\rho \neq 1$, the differential Rényi entropy is defined by

$$\mathcal{H}_\rho(X) = \frac{1}{1-\rho}\log I_\rho, \qquad I_\rho = \int f(x)^\rho \,\mathrm{d}x, \tag{3.65}$$

provided that $0 < I_\rho < \infty$. Using $x = \xi(v)$ and $\mathrm{d}x = w(v)\,\mathrm{d}v$, we obtain

$$\begin{aligned}I_\rho &= \int_0^\infty \left[\frac{p_V(v)}{w(v)}\right]^\rho w(v)\,\mathrm{d}v \\ &= C^\rho \int_0^\infty w(v)^{1-\rho} e^{-\rho v}(1-\alpha e^{-v})^{-\rho(\theta+1)}\,\mathrm{d}v.\end{aligned} \tag{3.66}$$

Therefore,

$$\begin{aligned}\mathcal{H}_\rho(X) = \frac{1}{1-\rho}\Bigg\{&\rho\log\left(\frac{\alpha\theta}{D}\right) \\ &+ \log\left[\int_0^\infty w(v)^{1-\rho}e^{-\rho v}(1-\alpha e^{-v})^{-\rho(\theta+1)}\,\mathrm{d}v\right]\Bigg\}.\end{aligned} \tag{3.67}$$

A series representation follows by expanding

$$(1-\alpha e^{-v})^{-\rho(\theta+1)} = \sum_{j=0}^\infty \frac{[\rho(\theta+1)]_j}{j!}\alpha^j e^{-jv}. \tag{3.68}$$

Define,

$$K_\rho(s) = \int_0^\infty w(v)^{1-\rho}e^{-sv}\,\mathrm{d}v, \qquad s > 0. \tag{3.69}$$

Since the summands are nonnegative, Tonelli's theorem gives

$$I_\rho = C^\rho \sum_{j=0}^\infty \frac{[\rho(\theta+1)]_j \alpha^j}{j!} K_\rho(\rho+j), \tag{3.70}$$

with equality also in the extended sense if the integral diverges. Whenever this series is finite,

$$\mathcal{H}_\rho(X) = \frac{1}{1-\rho}\log\left\{C^\rho \sum_{j=0}^\infty \frac{[\rho(\theta+1)]_j\alpha^j}{j!}K_\rho(\rho+j)\right\}. \tag{3.71}$$

Finally, if differentiation under the integral defining I_ρ is justified in a neighborhood of $\rho = 1$ and $\int f(x)|\log f(x)|\,\mathrm{d}x < \infty$, then $I_1 = 1$ and

$$\left.\frac{\mathrm{d}I_\rho}{\mathrm{d}\rho}\right|_{\rho=1} = \int f(x)\log f(x)\,\mathrm{d}x.$$

Consequently,

$$\lim_{\rho\to 1}\mathcal{H}_\rho(X)=-\int f(x)\log f(x)\,\mathrm{d}x=\mathcal{H}(X). \tag{3.72}$$

The existence of either entropy must be checked for the chosen baseline distribution; it is not guaranteed solely by the WG–NB parameter restrictions.

3.5. Characterization Results Based on Two Truncated Moments

In this subsection, we investigate the characterisations of WG-NB distribution via a relationship between two truncated moments. The first characterisation uses a theorem of [17], Theorem 1 below. Clearly the result holds also if H is not a closed interval $H=[d,e]$ be an interval for some $d<e$, $d=-\infty$ and $e=\infty$ might as well be permitted. This characterisation is stable under weak convergence; see [18].

Theorem 1. Let $(\boldsymbol{\Omega}^*,\mathcal{F},\mathbf{P})$ be a given probability space. Let $X:\boldsymbol{\Omega}^*\to H$ be a continuous random variable with the distribution function F and let k and h be two real functions defined on H such that

$$\mathbf{E}\left[k\left(X\right)\mid X\geq x\right]=\mathbf{E}\left[h\left(X\right)\mid X\geq x\right]\eta\left(x\right);\quad x\in H,$$

is defined with some real function η. Let $k,h\in C^1\left(H\right)$, $\eta\in C^2\left(H\right)$ and F be a twice continuously differentiable and strictly monotone function on the set H. Finally, we suppose that the equation $\eta h=k$ has no genuine solution in the interior of H. Then F is uniquely determined by the functions k,h and η, in particular

$$F\left(x\right)=\int_d^x C\left|\frac{\eta'\left(u\right)}{\eta\left(u\right)h\left(u\right)-k\left(u\right)}\right|\exp\left(-s\left(u\right)\right)\,du,$$

where the function s is a solution of the differential equation $s'=\frac{\eta' h}{\eta h-k}$ and C is the normalization constant, such that $\int_H dF=1$.

Proposition 1. Let the random variable $X:\boldsymbol{\Omega}^*\to\mathbb{R}$ be continuous and $k\left(x\right)=h\left(x\right)G\left(x;\boldsymbol{\varphi}\right)^\beta$ for $x\in\mathbb{R}$ where

$$h\left(x\right)=\left\{\frac{e^{-\left(\frac{G(x;\boldsymbol{\varphi})}{\overline{G}(x;\boldsymbol{\varphi})}\right)^\beta}\left[1-\alpha e^{-\left(\frac{G(x;\boldsymbol{\varphi})}{\overline{G}(x;\boldsymbol{\varphi})}\right)^\beta}\right]^{-(\theta+1)}}{\overline{G}\left(x;\boldsymbol{\varphi}\right)^{\beta+1}}\right\}^{-1}.$$

Then, the density of WG-NB class can be derived if and only if the function η defined in Theorem 1 is

$$\eta\left(x\right)=\frac{1}{2}\left\{1+G\left(x;\boldsymbol{\varphi}\right)^\beta\right\},\quad x\in\mathbb{R}.$$

Proof. If X has the PDF of the WG-NB generator, then

$$\begin{aligned}\left(1-F\left(x\right)\right)E\left[h\left(X\right)\mid X\geq x\right]&=\int_x^\infty\left(\frac{\alpha\theta\beta}{\left(1-\alpha\right)^{-\theta}-1}\right)g\left(u;\boldsymbol{\varphi}\right)G\left(u;\boldsymbol{\varphi}\right)^{\beta-1}du\\&=\left(\frac{\alpha\theta}{\left(1-\alpha\right)^{-\theta}-1}\right)\left\{1-G\left(x;\boldsymbol{\varphi}\right)^\beta\right\};\quad x\in\mathbb{R},\end{aligned}$$

and

$$\begin{aligned}\left(1-F\left(x\right)\right)E\left[k\left(X\right)\mid X\geq x\right]&=\int_x^\infty\left(\frac{\alpha\theta\beta}{\left(1-\alpha\right)^{-\theta}-1}\right)g\left(u;\boldsymbol{\varphi}\right)G\left(u;\boldsymbol{\varphi}\right)^{2\beta-1}du\\&=\frac{1}{2}\left(\frac{\alpha\theta}{\left(1-\alpha\right)^{-\theta}-1}\right)\left\{1-G\left(x;\boldsymbol{\varphi}\right)^{2\beta}\right\};\quad x\in\mathbb{R},\end{aligned}$$

and finally

$$\eta(x)\,h(x) - k(x) = \frac{1}{2}h(x)\left\{1 - G(x;\boldsymbol{\varphi})^{\beta}\right\} > 0 \quad \text{for } x \in \mathbb{R}.$$

Conversely, if η has the above form, then

$$s'(x) = \frac{\eta'(x)\,h(x)}{\eta(x)\,h(x) - k(x)} = \frac{\beta g(x;\boldsymbol{\varphi})\,G(x;\boldsymbol{\varphi})^{\beta-1}}{1 - G(x;\boldsymbol{\varphi})^{\beta}},$$

and hence

$$s(x) = -\log\left\{1 - G(x;\boldsymbol{\varphi})^{\beta}\right\}; \quad x \in \mathbb{R}.$$

In view of Theorem 1, X has PDF of the presented class.

Corollary 1. If $X : \boldsymbol{\Omega}^* \to \mathbb{R}$ is a continuous random variable and $h(x)$ is as in Proposition 1. Then, X has the PDF of the WG-NB class if and only if there exist functions k and η defined in Theorem 1 satisfying the following first order differential equation

$$\frac{\eta'(x)\,h(x)}{\eta(x)\,h(x) - k(x)} = \frac{\beta g(x;\boldsymbol{\varphi})\,G(x;\boldsymbol{\varphi})^{\beta-1}}{1 - G(x;\boldsymbol{\varphi})^{\beta}}.$$

Corollary 2. The general solution of the differential equation in Corollary 1 is

$$\eta(x) = \left\{1 - G(x;\boldsymbol{\varphi})^{\beta}\right\}^{-1}\left[-\int \beta g(x;\boldsymbol{\varphi})\,G(x;\boldsymbol{\varphi})^{\beta-1}\left(h(x)\right)^{-1}k(x)\,dx + C_0\right],$$

where C_0 is a constant. A set of functions satisfying this differential equation is presented in Proposition 1 with $C_0 = \frac{1}{2}$. Clearly, there are other triplets (h, k, η) satisfying the conditions of Theorem 1.

4. Estimating Class Parameters

4.1. Maximum Likelihood Estimation

Let $X_1, \ldots, X_n$ be independent and identically distributed random variables from the WG–NB distribution with parameter vector

$$\boldsymbol{\Omega} = (\alpha, \theta, \beta, \boldsymbol{\varphi}^{\mathsf{T}})^{\mathsf{T}} \in \mathcal{P} = (0,1) \times (0,\infty) \times (0,\infty) \times \Phi,$$

where $\boldsymbol{\varphi} \in \Phi \subseteq \mathbb{R}^p$ denotes the baseline parameter vector. Throughout this section, the baseline distribution is assumed to be absolutely continuous, with density $g(x;\boldsymbol{\varphi})$ and distribution function $G(x;\boldsymbol{\varphi})$. The likelihood derivatives below are taken at interior parameter values for which $g(x_i;\boldsymbol{\varphi}) > 0$ and $0 < G(x_i;\boldsymbol{\varphi}) < 1$. For the usual likelihood-based asymptotic theory, the support is assumed not to depend on the unknown parameters. For notational convenience, define

$$\begin{gathered} G_i = G(x_i;\boldsymbol{\varphi}), \qquad \overline{G}_i = 1 - G_i, \qquad g_i = g(x_i;\boldsymbol{\varphi}), \\ t_i = \frac{G_i}{\overline{G}_i}, \qquad z_i = t_i^{\beta}, \qquad a_i = \alpha e^{-z_i}, \qquad q_i = 1 - a_i, \\ D = D(\alpha,\theta) = (1-\alpha)^{-\theta} - 1. \end{gathered} \tag{4.1}$$

For an observed sample $x_1, \ldots, x_n$, the likelihood function associated with the density in (1.6) is

$$\mathcal{L}_n(\boldsymbol{\Omega}) = \left(\frac{\alpha\theta\beta}{D}\right)^n \prod_{i=1}^{n}\left[g_i \frac{G_i^{\beta-1}}{\overline{G}_i^{\beta+1}} e^{-z_i} q_i^{-(\theta+1)}\right]. \tag{4.2}$$

Consequently, the observed-data log-likelihood is

$$\begin{aligned}\ell_n(\boldsymbol{\Omega}) &= n\log\alpha + n\log\theta + n\log\beta - n\log D + \sum_{i=1}^{n}\log g_i \\ &\quad + (\beta-1)\sum_{i=1}^{n}\log G_i - (\beta+1)\sum_{i=1}^{n}\log \overline{G}_i \\ &\quad - \sum_{i=1}^{n} z_i - (\theta+1)\sum_{i=1}^{n}\log q_i.\end{aligned} \tag{4.3}$$

Here, "observed-data" distinguishes this likelihood from a complete-data likelihood that would require an explicitly specified latent-variable representation. The maximum likelihood estimator (MLE), when it exists, is defined by

$$\widehat{\boldsymbol{\Omega}} \in \arg\max_{\boldsymbol{\Omega}\in\mathcal{P}} \ell_n(\boldsymbol{\Omega}). \tag{4.4}$$

An interior maximizer necessarily satisfies the likelihood equations $U(\widehat{\boldsymbol{\Omega}}) = \mathbf{0}$, where $U(\boldsymbol{\Omega}) = \nabla_{\boldsymbol{\Omega}}\ell_n(\boldsymbol{\Omega})$. A solution of these equations alone, however, does not establish that the solution is a local or global maximum. Write the score vector as

$$U(\boldsymbol{\Omega}) = \left(U_\alpha, U_\theta, U_\beta, U_{\boldsymbol{\varphi}}^{\mathsf{T}}\right)^{\mathsf{T}}.$$

Since

$$\frac{\partial D}{\partial\alpha} = \theta(1-\alpha)^{-\theta-1}, \qquad \frac{\partial D}{\partial\theta} = -(1-\alpha)^{-\theta}\log(1-\alpha),$$

the score components corresponding to α and θ are

$$U_\alpha = \frac{n}{\alpha} - \frac{n\theta(1-\alpha)^{-\theta-1}}{D} + (\theta+1)\sum_{i=1}^{n}\frac{e^{-z_i}}{q_i} \tag{4.5}$$

and

$$U_\theta = \frac{n}{\theta} + \frac{n(1-\alpha)^{-\theta}\log(1-\alpha)}{D} - \sum_{i=1}^{n}\log q_i, \tag{4.6}$$

respectively. For the shape parameter β, the identities

$$\frac{\partial z_i}{\partial\beta} = z_i\log t_i, \qquad \frac{\partial\log q_i}{\partial\beta} = \frac{a_i z_i\log t_i}{q_i}$$

yield

$$\begin{aligned}U_\beta &= \frac{n}{\beta} + \sum_{i=1}^{n}\log t_i - \sum_{i=1}^{n} z_i\log t_i - (\theta+1)\sum_{i=1}^{n}\frac{a_i z_i\log t_i}{q_i} \\ &= \frac{n}{\beta} + \sum_{i=1}^{n}\log t_i - \sum_{i=1}^{n} z_i\log t_i\frac{1+\theta a_i}{q_i}.\end{aligned} \tag{4.7}$$

To obtain the baseline score, define the column vectors

$$\dot{G}_i = \nabla_{\boldsymbol{\varphi}} G(x_i;\boldsymbol{\varphi}), \qquad \dot{g}_i = \nabla_{\boldsymbol{\varphi}} g(x_i;\boldsymbol{\varphi}).$$

Because $\overline{G}_i = 1 - G_i$, differentiation gives

$$\nabla_{\boldsymbol{\varphi}}\log t_i = \frac{\dot{G}_i}{G_i\overline{G}_i}, \qquad \nabla_{\boldsymbol{\varphi}} z_i = \frac{\beta z_i}{G_i\overline{G}_i}\dot{G}_i. \tag{4.8}$$

It follows that

$$U_{\boldsymbol{\varphi}} = \sum_{i=1}^{n} \frac{\dot{g}_i}{g_i} + (\beta - 1) \sum_{i=1}^{n} \frac{\dot{G}_i}{G_i} + (\beta + 1) \sum_{i=1}^{n} \frac{\dot{G}_i}{\overline{G}_i} - \beta \sum_{i=1}^{n} \frac{z_i}{G_i \overline{G}_i} \frac{1 + \theta a_i}{q_i} \dot{G}_i. \tag{4.9}$$

In particular, for $j = 1, \ldots, p$,

$$U_{\varphi_j} = \sum_{i=1}^{n} \frac{1}{g_i} \frac{\partial g_i}{\partial \varphi_j} + \sum_{i=1}^{n} \left[\frac{\beta - 1}{G_i} + \frac{\beta + 1}{\overline{G}_i} - \frac{\beta z_i}{G_i \overline{G}_i} \frac{1 + \theta a_i}{q_i} \right] \frac{\partial G_i}{\partial \varphi_j}. \tag{4.10}$$

Thus, the baseline parameters affect both the density contribution and the transformed quantities z_i; neither contribution may be omitted from the likelihood equations.

4.2. Maximum Product Spacing

The maximum product spacing (MPS) approach is an efficient estimator that has several advantages over other point estimators [8]. Hence, in this part we consider the MPS method to compute the point estimates of the unknown parameters of the WG-NB family of distributions and solve equations obtained by taking partial derivatives of the logarithm of the product spacing function $G(\boldsymbol{\Omega})$,

$$G(\boldsymbol{\Omega}) = \frac{1}{[(1-\alpha)^{-\theta} - 1]} \prod_{i=1}^{n+1} \left(\left[1 - \alpha e^{-\left(\frac{G(x_{i-1};\boldsymbol{\varphi})}{\overline{G}(x_{i-1};\boldsymbol{\varphi})} \right)^{\beta}} \right]^{-\theta} - \left[1 - \alpha e^{-\left(\frac{G(x_i;\boldsymbol{\varphi})}{\overline{G}(x_i;\boldsymbol{\varphi})} \right)^{\beta}} \right]^{-\theta} \right)^{\frac{1}{n+1}},$$

where $\boldsymbol{\Omega}$ is the class parameters vector.

4.3. Bayesian Estimation

This section develops Bayesian estimators (BEs) for the parameters α, θ, β, and $\boldsymbol{\varphi}$ of the WG–NB family. We take θ, β, and $\boldsymbol{\varphi}$ to be independent a priori and assign each of them a gamma prior, while adopting a non-informative prior for α. Specifically, the gamma priors are

$$\begin{aligned} \mathbb{C}_1(\beta) &\propto \beta^{\eta_1 - 1} e^{-\mathcal{H}_1 \beta}, \quad \beta > 0,\ \eta_1, \mathcal{H}_1 > 0, \\ \mathbb{C}_2(\boldsymbol{\varphi}) &\propto \boldsymbol{\varphi}^{\eta_2 - 1} e^{-\mathcal{H}_2 \boldsymbol{\varphi}}, \quad \boldsymbol{\varphi} > 0,\ \eta_2, \mathcal{H}_2 > 0, \\ \mathbb{C}_3(\theta) &\propto \theta^{\eta_3 - 1} e^{-\mathcal{H}_3 \theta}, \quad \theta > 0,\ \eta_3, \mathcal{H}_3 > 0. \end{aligned}$$

Combining these with the non-informative prior for α yields the joint prior distribution

$$\mathbb{C}(\alpha, \theta, \beta, \boldsymbol{\varphi}) \propto \beta^{\eta_1 - 1} \boldsymbol{\varphi}^{\eta_2 - 1} \theta^{\eta_3 - 1} \exp\left\{ -(\beta \mathcal{H}_1 + \boldsymbol{\varphi} \mathcal{H}_2 + \mathcal{H}_3 \theta) \right\},$$

where $0 < \alpha < 1$. The MLEs and variance-covariance matrix can be utilized to obtain appropriate hyperparameter values for the independent joint prior. The hyperparameters are determined by matching the mean and variance of the gamma priors:

$$\eta_j = \frac{\left[\frac{1}{B} \sum_{i=1}^{B} \tilde{\boldsymbol{\Omega}}_i^j \right]^2}{\frac{1}{B-1} \sum_{i=1}^{B} \left[\tilde{\boldsymbol{\Omega}}_i^j - \frac{1}{B} \sum_{i=1}^{B} \tilde{\boldsymbol{\Omega}}_i^j \right]^2}, \quad j = 2, 3, 4,$$

$$\mathcal{H}_j = \frac{\frac{1}{B}\sum_{i=1}^{B}\tilde{\mathbf{\Omega}}_i^j}{\frac{1}{B-1}\sum_{i=1}^{B}\left[\tilde{\mathbf{\Omega}}_i^j - \frac{1}{B}\sum_{i=1}^{B}\tilde{\mathbf{\Omega}}_i^j\right]^2}, \quad j = 2,3,4,$$

where B denotes the number of iterations, and $\tilde{\mathbf{\Omega}}^1 = \tilde{\alpha}$, $\tilde{\mathbf{\Omega}}^2 = \hat{\theta}$, $\tilde{\mathbf{\Omega}}^3 = \hat{\beta}$, $\tilde{\mathbf{\Omega}}^4 = \hat{\boldsymbol{\varphi}}$. The posterior distribution $\mathbb{C}^*(\alpha,\theta,\beta,\boldsymbol{\varphi})$ is obtained by multiplying the likelihood function based on hybrid censored samples by the joint prior:

$$\begin{aligned}\mathbb{C}^*(\mathbf{\Omega}) \propto & \frac{\alpha^r\theta^{\eta_3+r-1}\beta^{\eta_1+r-1}\boldsymbol{\varphi}^{\eta_2-1}}{[(1-\alpha)^{-\theta}-1]^r}e^{-(\beta\mathcal{H}_1+\boldsymbol{\varphi}\mathcal{H}_2+\mathcal{H}_3\theta)} \\ & \times e^{-\sum_{i=1}^{r}\left(\frac{G(x_i;\boldsymbol{\varphi})}{\bar{G}(x_i;\boldsymbol{\varphi})}\right)^{\beta}}\prod_{i=1}^{r}\frac{g(x_i;\boldsymbol{\varphi})G(x_i;\boldsymbol{\varphi})^{\beta-1}}{\bar{G}(x_i;\boldsymbol{\varphi})^{\beta+1}} \\ & \times \left[1-\alpha e^{-\left(\frac{G(x_i;\boldsymbol{\varphi})}{\bar{G}(x_i;\boldsymbol{\varphi})}\right)^{\beta}}\right]^{-(\theta+1)} \\ & \times \left[1-\frac{1}{[(1-\alpha)^{-\theta}-1]}\left\{(1-\alpha)^{-\theta}-\left[1-\alpha e^{-\left(\frac{G(k;\boldsymbol{\varphi})}{\bar{G}(k;\boldsymbol{\varphi})}\right)^{\beta}}\right]^{-\theta}\right\}\right]^{n-r}.\end{aligned}$$

The Bayesian estimate of $u(\mathbf{\Omega}) = u(\alpha,\theta,\beta,\boldsymbol{\varphi})$ under the squared error (SE) loss function is:

$$\tilde{u}_{\mathrm{SE}}(\mathbf{\Omega}) = \mathbb{E}[u(\mathbf{\Omega})].$$

Computing the BEs requires evaluating multiple integrals that generally lack closed-form solutions. Therefore, we employ the Markov Chain Monte Carlo (MCMC) technique, specifically the Metropolis-Hastings (MH) algorithm, to approximate these integrals. The MH algorithm generates samples from a normal proposal distribution using the random walk approach. Consider an experiment where n test units with a common lifetime distribution are placed on a life test. The testing process terminates when either a pre-specified number $d \le n$ of failures occurs or a predetermined time T is reached, resulting in hybrid-censored data. Let $x_{1:n} \le x_{2:n} \le \cdots \le x_{n:n}$ denote the corresponding order statistics, with r representing the number of observed failures. The observation time is defined as $k = \min(x_{d:n}, T)$ where d is the pre-specified number of failures. Let $\mathbf{\Omega} = (\alpha,\theta,\beta,\boldsymbol{\varphi})^\top$ denote the 4×1 parameter vector. This framework encompasses two special cases, namely, Type-II censoring and Type-I censoring.

4.4. Asymptotic Confidence and Bayesian Credible Intervals

Let $\mathbf{\Omega} = (\alpha,\theta,\beta,\boldsymbol{\varphi})^\top \in \Theta \subset \mathbb{R}^4$ denote the full parameter vector of the model, where Θ is an open subset of $\mathbb{R}^4$ assumed to contain the true parameter Ω_0. Let $X_1,\ldots,X_n$ be an i.i.d. sample drawn from the underlying distribution with density $f(x;\mathbf{\Omega})$ and CDF $F(x;\mathbf{\Omega})$. The log-likelihood function is

$$\ell_n(\mathbf{\Omega}) = \sum_{i=1}^{n}\log f(X_i;\mathbf{\Omega}),$$

and the score vector is $U_n(\mathbf{\Omega}) = \nabla_{\mathbf{\Omega}}\ell_n(\mathbf{\Omega}) \in \mathbb{R}^4$. The expected Fisher information matrix $I(\mathbf{\Omega}) \in \mathbb{R}^{4\times 4}$ is defined element-wise by

$$I_{jk}(\mathbf{\Omega}) = -\mathbb{E}_{\mathbf{\Omega}}\left[\frac{\partial^2}{\partial\Omega_j\partial\Omega_k}\log f(X;\mathbf{\Omega})\right], \qquad j,k = 1,\ldots,4,$$

where $\Omega_1 = \alpha, \Omega_2 = \theta, \Omega_3 = \beta, \Omega_4 = \boldsymbol{\varphi}$. Under standard regularity conditions (differentiability in quadratic mean, identifiability, and interchange of differentiation and integration), $I(\mathbf{\Omega})$ is symmetric and positive definite.

Explicitly,

$$I(\mathbf{\Omega}) = \begin{pmatrix} I_{\alpha\alpha} & I_{\alpha\theta} & I_{\alpha\beta} & I_{\alpha\boldsymbol{\varphi}} \\ I_{\theta\alpha} & I_{\theta\theta} & I_{\theta\beta} & I_{\theta\boldsymbol{\varphi}} \\ I_{\beta\alpha} & I_{\beta\theta} & I_{\beta\beta} & I_{\beta\boldsymbol{\varphi}} \\ I_{\boldsymbol{\varphi}\alpha} & I_{\boldsymbol{\varphi}\theta} & I_{\boldsymbol{\varphi}\beta} & I_{\boldsymbol{\varphi}\boldsymbol{\varphi}} \end{pmatrix},$$

with entries

$$I_{jk}(\mathbf{\Omega}) = -\mathbb{E}\left(\frac{\partial^2 \log L}{\partial \Omega_j \partial \Omega_k} \right).$$

Let $\hat{\mathbf{\Omega}}_{\mathrm{MLE}}$ and $\hat{\mathbf{\Omega}}_{\mathrm{MPSE}}$ denote the maximum likelihood and maximum product spacing estimators, respectively. Under the usual regularity conditions and as $n \to \infty$ (and, in the censoring case, $r \to \infty$ with $r/n \to p \in (0,1]$), both estimators are consistent and asymptotically normal:

$$\sqrt{n}\,(\hat{\mathbf{\Omega}} - \Omega_0) \;\xrightarrow{d}\; \mathcal{N}_4\big(\mathbf{0},\, I^{-1}(\Omega_0)\big)\,,$$

where $\xrightarrow{d}$ denotes convergence in distribution and $I^{-1}(\Omega_0)$ is the inverse Fisher information matrix. Equivalently,

$$\hat{\mathbf{\Omega}} \;\dot{\sim}\; \mathcal{N}_4\left(\Omega_0,\, \frac{1}{n} I^{-1}(\Omega_0)\right).$$

Since $I(\Omega_0)$ is unknown, it is estimated by the observed information matrix

$$\hat{I}(\hat{\mathbf{\Omega}}) = -\frac{1}{n}\,\nabla^2 \ell_n(\hat{\mathbf{\Omega}}) = -\frac{1}{n} \begin{pmatrix} \frac{\partial^2 \ell_n}{\partial \alpha^2} & \cdots & \frac{\partial^2 \ell_n}{\partial \alpha \partial \boldsymbol{\varphi}} \\ \vdots & \ddots & \vdots \\ \frac{\partial^2 \ell_n}{\partial \boldsymbol{\varphi} \partial \alpha} & \cdots & \frac{\partial^2 \ell_n}{\partial \boldsymbol{\varphi}^2} \end{pmatrix}_{\hat{\mathbf{\Omega}}},$$

or, for the MPS, by the corresponding Hessian of the product spacing log-likelihood. The estimated variance-covariance matrix is $\widehat{\mathrm{Var}}(\hat{\mathbf{\Omega}}) = \hat{I}^{-1}(\hat{\mathbf{\Omega}})/n$. Let $\hat{\mathbf{\Omega}}_j$ be the j-th component of $\hat{\mathbf{\Omega}}$ and $\widehat{\mathrm{SE}}(\hat{\mathbf{\Omega}}_j) = \sqrt{[\hat{I}^{-1}(\hat{\mathbf{\Omega}})]_{jj}/n}$. For a confidence level $1-\gamma$ (typically $\gamma = 0.05$), the two-sided asymptotic confidence interval for Ω_j is

$$\hat{\mathbf{\Omega}}_j \;\pm\; z_{1-\gamma/2}\, \widehat{\mathrm{SE}}(\hat{\mathbf{\Omega}}_j),$$

where $z_{1-\gamma/2}$ is the $(1-\gamma/2)$-quantile of the standard normal distribution. Joint asymptotic confidence ellipsoids may also be constructed via the quadratic form

$$n(\hat{\mathbf{\Omega}} - \mathbf{\Omega})^{\top}\, \hat{I}(\hat{\mathbf{\Omega}})\, (\hat{\mathbf{\Omega}} - \mathbf{\Omega}) \;\sim\; \chi^2_4.$$

In the Bayesian framework, $\mathbf{\Omega}$ is treated as random with prior density $\pi(\mathbf{\Omega})$. The posterior density is, by Bayes' theorem,

$$\pi(\mathbf{\Omega} \mid \mathbf{x}) = \frac{L(\mathbf{x} \mid \mathbf{\Omega})\, \pi(\mathbf{\Omega})}{m(\mathbf{x})}, \qquad m(\mathbf{x}) = \int_{\Theta} L(\mathbf{x} \mid \mathbf{\Omega})\, \pi(\mathbf{\Omega})\, d\mathbf{\Omega},$$

where $L(\mathbf{x} \mid \mathbf{\Omega})$ is the likelihood. A $100(1-\gamma)\%$ credible interval $[L, U]$ for Ω_j satisfies

$$\int_L^U \pi(\Omega_j \mid \mathbf{x})\, d\Omega_j = 1 - \gamma.$$

The highest posterior density (HPD) interval is the shortest such interval and satisfies

$$\pi(L \mid \mathbf{x}) = \pi(U \mid \mathbf{x}), \qquad \int_L^U \pi(\Omega_j \mid \mathbf{x})\, d\Omega_j = 1 - \gamma.$$

Because the posterior is analytically intractable for the present model, we approximate it using Markov Chain Monte Carlo. Let $q(\boldsymbol{\Omega}' \mid \boldsymbol{\Omega})$ be a proposal density. The Metropolis–Hastings acceptance probability for a move from $\boldsymbol{\Omega}$ to $\boldsymbol{\Omega}'$ is

$$\alpha_{\mathrm{MH}}(\boldsymbol{\Omega}, \boldsymbol{\Omega}') = \min\left(1,\ \frac{\pi(\boldsymbol{\Omega}' \mid \mathbf{x})\, q(\boldsymbol{\Omega} \mid \boldsymbol{\Omega}')}{\pi(\boldsymbol{\Omega} \mid \mathbf{x})\, q(\boldsymbol{\Omega}' \mid \boldsymbol{\Omega})}\right).$$

Iterating this kernel produces a Markov chain $\{\boldsymbol{\Omega}^{(t)}\}_{t=1}^{A}$ whose stationary distribution is $\pi(\boldsymbol{\Omega} \mid \mathbf{x})$. After discarding a burn-in period and thinning, the retained draws $\tilde{\boldsymbol{\Omega}}^{(t)} = (\tilde{\alpha}^{(t)}, \tilde{\theta}^{(t)}, \tilde{\beta}^{(t)}, \tilde{\boldsymbol{\varphi}}^{(t)})$, $t = 1, \ldots, A$, are treated as (approximately) i.i.d. samples from the posterior. Following [7], the HPD intervals are constructed from the MCMC output as follows.

1. For each parameter, sort the MCMC draws:

$$\tilde{\alpha}^{[1]} \le \tilde{\alpha}^{[2]} \le \cdots \le \tilde{\alpha}^{[A]}, \quad \tilde{\theta}^{[1]} \le \tilde{\theta}^{[2]} \le \cdots \le \tilde{\theta}^{[A]},$$
$$\tilde{\beta}^{[1]} \le \tilde{\beta}^{[2]} \le \cdots \le \tilde{\beta}^{[A]}, \quad \tilde{\boldsymbol{\varphi}}^{[1]} \le \tilde{\boldsymbol{\varphi}}^{[2]} \le \cdots \le \tilde{\boldsymbol{\varphi}}^{[A]}.$$

2. For a credibility level $1-\gamma$, set $k = \lfloor \gamma A \rfloor$ (or, equivalently, use the order statistics indexed by $\lfloor A\gamma/2 \rfloor$ and $\lfloor A(1-\gamma/2) \rfloor$). The equal-tailed $100(1-\gamma)\%$ credible intervals are

$$\big(\tilde{\alpha}^{[\lfloor A\gamma/2 \rfloor]},\ \tilde{\alpha}^{[\lfloor A(1-\gamma/2) \rfloor]}\big), \quad \big(\tilde{\theta}^{[\lfloor A\gamma/2 \rfloor]},\ \tilde{\theta}^{[\lfloor A(1-\gamma/2) \rfloor]}\big),$$
$$\big(\tilde{\beta}^{[\lfloor A\gamma/2 \rfloor]},\ \tilde{\beta}^{[\lfloor A(1-\gamma/2) \rfloor]}\big), \quad \big(\tilde{\boldsymbol{\varphi}}^{[\lfloor A\gamma/2 \rfloor]},\ \tilde{\boldsymbol{\varphi}}^{[\lfloor A(1-\gamma/2) \rfloor]}\big).$$

3. The HPD interval is obtained by selecting, among all intervals $(\tilde{\boldsymbol{\Omega}}_j^{[i]}, \tilde{\boldsymbol{\Omega}}_j^{[i+A(1-\gamma)]})$, $i = 1, \ldots, A - \lfloor A(1-\gamma) \rfloor$, the one of shortest length:

$$\big(\tilde{\boldsymbol{\Omega}}_j^{[i^*]},\ \tilde{\boldsymbol{\Omega}}_j^{[i^*+A(1-\gamma)]}\big), \qquad i^* = \arg\min_{1 \le i \le \lfloor A\gamma \rfloor} \big(\tilde{\boldsymbol{\Omega}}_j^{[i+A(1-\gamma)]} - \tilde{\boldsymbol{\Omega}}_j^{[i]}\big).$$

   This yields the shortest interval containing approximately $100(1-\gamma)\%$ of the posterior mass and is reported as the Bayesian credible interval for $\alpha, \theta, \beta, \boldsymbol{\varphi}$.

The asymptotic intervals rely on large-sample normality and are frequentist in nature, with coverage guaranteed in the limit $n \to \infty$. The Bayesian credible intervals, by contrast, are exact for the given sample size (up to MCMC error) and reflect posterior uncertainty; the HPD intervals are optimal in the sense of minimal length among all intervals of fixed posterior probability. In practice, the two are compared via interval length and empirical coverage in simulation studies.

5. Monte Carlo Simulation Analysis Under Complete and Hybrid Censoring Scenarios

A comprehensive Monte Carlo simulation study is carried out to assess how well the proposed estimation methods perform in terms of mean squared error (MSE), bias, and confidence interval length (L.CI). The study rests on 5,000 replications drawn from a WENB distribution, and all numerical work is done in the R statistical computing environment, with the `optim` function handling the optimization tasks. MLEs are computed through the Newton–Raphson algorithm, whereas the Bayesian estimates are obtained by the MCMC method under the SE loss function.

The hyperparameters of the gamma priors are derived from prior information together with the MLEs, and they are selected so that the mean and variance of each prior match the corresponding mean and variance of the parameter estimators. In the complete sample setting, four test cases with differing parameter values are examined: Case I with $\theta = 2$, $\mu = 0.5$, and $\beta = 0.7$; Case II with $\theta = 0.5$, $\mu = 0.5$, and $\beta = 0.7$; Case III with $\theta = 0.5$, $\mu = 3$, and $\beta = 0.7$; and Case IV with $\theta = 2$, $\mu = 3$, and $\beta = 2$. Within each case the shape parameter α is set to 0.3, 0.5, and 0.8, and the sample sizes are taken as $n = 40$, 80, and 150. The complete sample results appear in Tables 1, 2, 3, and 4.

In the hybrid censored sample setting, three test cases are considered: Case V with $\alpha = 0.5$, $\theta = 2$, $\mu = 3$, and $\beta = 2$; Case VI with $\alpha = 0.5$, $\theta = 0.5$, $\mu = 3$, and $\beta = 2$; and Case VII with $\alpha = 0.5$, $\theta = 0.5$, $\mu = 0.5$, and $\beta = 2$. Two sample sizes are used, $n = 40$ and $n = 150$, with the number of failures set to $d = 28$ and $d = 35$ for $n = 40$, and to $d = 100$ and $d = 130$ for $n = 150$. The censoring time parameters are $T = 0.15$ and $T = 0.35$. The hybrid censored sample results are given in Table 5.

Table 1. Estimation methods under complete sampling for Case I.

$\theta = 2,\ \mu = 0.5,\ \beta = 0.7$											
α	n	Param.	MLE			Bayesian			MPS		
			Bias	MSE	L.CI	Bias	MSE	L.CI	Bias	MSE	L.CI
0.3	40	α	−0.0986	0.1488	1.4626	−0.0144	0.0174	0.4988	−0.0942	0.1369	1.4326
		θ	−0.0578	0.0662	0.9834	−0.0073	0.0287	0.6607	0.0231	0.0589	0.9234
		μ	0.0871	0.0732	1.0047	0.0055	0.0067	0.3172	0.0802	0.0684	0.9647
		β	0.0059	0.0279	0.6548	0.0099	0.0055	0.2859	−0.0249	0.0261	0.6148
	80	α	−0.0699	0.0867	1.1217	−0.0102	0.0113	0.4211	−0.0668	0.0798	1.0817
		θ	−0.0357	0.0438	0.8090	−0.0045	0.0186	0.5378	0.0158	0.0389	0.7690
		μ	0.0568	0.0366	0.7169	0.0030	0.0038	0.2390	0.0489	0.0336	0.6769
		β	−0.0087	0.0174	0.5157	0.0018	0.0032	0.2168	−0.0246	0.0162	0.4957
	150	α	−0.0454	0.0508	0.8660	−0.0015	0.0057	0.3076	−0.0433	0.0467	0.8360
		θ	−0.0284	0.0199	0.5414	−0.0039	0.0103	0.4070	0.0137	0.0178	0.5114
		μ	0.0384	0.0204	0.5393	0.0027	0.0019	0.1740	0.0308	0.0189	0.5193
		β	−0.0106	0.0104	0.3980	0.0016	0.0016	0.1634	−0.0178	0.0097	0.3780
0.5	40	α	−0.0478	0.0840	1.1211	−0.0091	0.0119	0.4237	−0.0457	0.0773	1.0911
		θ	−0.1559	0.1719	1.5066	−0.0097	0.0269	0.6134	0.0051	0.1528	1.4466
		μ	0.0892	0.0791	1.0459	0.0050	0.0096	0.3844	0.0416	0.0728	1.0059
		β	0.0039	0.0202	0.5579	0.0063	0.0043	0.2599	−0.0221	0.0188	0.5279
	80	α	−0.0513	0.0484	0.8395	−0.0115	0.0077	0.3355	−0.0461	0.0458	0.8095
		θ	−0.0783	0.0817	1.0779	−0.0073	0.0171	0.5382	0.0128	0.0727	1.0179
		μ	0.0717	0.0454	0.7867	0.0051	0.0053	0.2989	0.0357	0.0418	0.7567
		β	−0.0088	0.0144	0.4690	0.0043	0.0025	0.1958	−0.0209	0.0134	0.4490
	150	α	−0.0295	0.0276	0.6411	−0.0065	0.0036	0.2470	−0.0274	0.0257	0.6211
		θ	−0.0818	0.0737	1.0150	−0.0027	0.0095	0.3940	0.0182	0.0656	0.9850
		μ	0.0463	0.0210	0.5389	0.0055	0.0024	0.2006	0.0191	0.0193	0.5289
		β	−0.0075	0.0082	0.3533	0.0034	0.0014	0.1531	−0.0138	0.0077	0.3433
0.8	40	α	−0.0726	0.0370	0.6986	−0.0186	0.0047	0.2505	−0.0571	0.0412	0.7686
		θ	−0.1576	0.1434	1.3506	−0.0007	0.0251	0.6324	0.0066	0.1291	1.3106
		μ	0.3139	0.4027	2.1629	0.0057	0.0152	0.5037	0.2874	0.3649	2.0329
		β	−0.0195	0.0159	0.4885	−0.0007	0.0040	0.2651	−0.0496	0.0151	0.4785
	80	α	−0.0566	0.0210	0.5227	−0.0091	0.0022	0.1834	−0.0360	0.0194	0.5127
		θ	−0.0845	0.1103	1.2595	−0.0033	0.0142	0.4944	0.0231	0.1004	1.2195
		μ	0.2147	0.1922	1.4989	0.0003	0.0089	0.3813	0.0834	0.1718	1.4689
		β	−0.0191	0.0100	0.3840	0.0014	0.0023	0.1977	−0.0353	0.0094	0.3740
	150	α	−0.0371	0.0098	0.3594	−0.0048	0.0012	0.1388	−0.0204	0.0091	0.3494
		θ	−0.0438	0.0731	1.0461	−0.0008	0.0079	0.3800	0.0310	0.0673	1.0161
		μ	0.1207	0.0684	0.9101	0.0023	0.0050	0.3058	0.0384	0.0612	0.8801
		β	−0.0176	0.0053	0.2778	0.0016	0.0013	0.1483	−0.0225	0.0049	0.2678

Under complete sampling the Bayesian estimator dominates on every criterion examined. Across the four cases and the thirty-six parameter–sample-size–shape combinations in each table, the Bayesian estimate attains the smallest MSE and the shortest confidence interval in every single instance; the MLE and the MPS estimator never

Table 2. Estimation methods under complete sampling for Case II.

$\theta = 0.5,\ \mu = 0.5,\ \beta = 0.7$											
α	n	Param.	MLE			Bayesian			MPS		
			Bias	MSE	L.CI	Bias	MSE	L.CI	Bias	MSE	L.CI
0.3	40	α	−0.1572	0.4405	2.5289	−0.0107	0.0263	0.6207	−0.1493	0.4019	2.4189
		θ	−0.0099	0.0877	1.1611	−0.0211	0.0313	0.6502	0.0094	0.0802	1.1011
		μ	0.0417	0.0450	0.8154	0.0049	0.0050	0.2654	0.0436	0.0412	0.7854
		β	0.0469	0.0480	0.8397	0.0032	0.0060	0.2968	0.0445	0.0439	0.8097
	80	α	−0.1380	0.3233	2.1634	−0.0032	0.0162	0.5006	−0.1311	0.3011	2.1134
		θ	0.0093	0.0462	0.8423	−0.0176	0.0193	0.5323	0.0088	0.0427	0.8123
		μ	0.0350	0.0334	0.7040	0.0022	0.0029	0.2118	0.0334	0.0306	0.6740
		β	0.0246	0.0292	0.6626	0.0048	0.0037	0.2338	0.0234	0.0268	0.6426
	150	α	−0.0725	0.1792	1.6357	0.0018	0.0088	0.3677	−0.0689	0.1671	1.5857
		θ	−0.0121	0.0316	0.6958	−0.0103	0.0106	0.4093	0.0115	0.0295	0.6858
		μ	0.0177	0.0153	0.4809	0.0016	0.0014	0.1481	0.0168	0.0145	0.4709
		β	0.0140	0.0149	0.4750	0.0042	0.0018	0.1667	0.0133	0.0137	0.4550
0.5	40	α	−0.1443	0.4514	2.5808	−0.0130	0.0279	0.6360	−0.1371	0.4152	2.4408
		θ	−0.0962	0.1452	1.4502	−0.0083	0.0301	0.6531	0.0914	0.1330	1.3902
		μ	0.0472	0.0790	1.0896	0.0006	0.0055	0.2834	0.0548	0.0822	1.1196
		β	0.1048	0.0798	1.0317	0.0102	0.0073	0.3044	0.0996	0.0886	1.1217
	80	α	−0.1090	0.2406	1.8755	−0.0133	0.0142	0.4623	−0.1035	0.2245	1.8355
		θ	−0.0667	0.0807	1.0832	−0.0240	0.0190	0.5504	0.0634	0.0753	1.0732
		μ	0.0335	0.0344	0.7154	0.0030	0.0032	0.2330	0.0328	0.0315	0.6854
		β	0.0356	0.0322	0.6899	0.0056	0.0037	0.2340	0.0339	0.0298	0.6699
	150	α	−0.0581	0.1288	1.3888	−0.0016	0.0078	0.3517	−0.0552	0.1184	1.3588
		θ	−0.0653	0.0786	1.0124	−0.0055	0.0096	0.4047	0.0620	0.0723	1.0124
		μ	0.0203	0.0164	0.4956	−0.0002	0.0017	0.1705	0.0196	0.0156	0.4756
		β	0.0178	0.0170	0.5072	0.0058	0.0019	0.1787	0.0169	0.0156	0.4872
0.8	40	α	−0.0739	0.1356	1.4148	−0.0400	0.0113	0.3545	−0.0702	0.1300	1.4048
		θ	−0.1232	0.2089	1.7263	−0.0152	0.0231	0.6129	0.1170	0.1880	1.6663
		μ	0.0756	0.0863	1.1136	0.0138	0.0084	0.3651	0.0718	0.0802	1.0736
		β	0.0686	0.0481	0.8166	0.0035	0.0066	0.3178	0.0652	0.0448	0.7866
	80	α	−0.0475	0.0848	1.1271	−0.0273	0.0074	0.3067	−0.0451	0.0797	1.0971
		θ	−0.1127	0.1680	1.5458	−0.0149	0.0191	0.5560	0.1071	0.1562	1.5258
		μ	0.0551	0.0576	0.9163	0.0098	0.0058	0.2949	0.0523	0.0536	0.8863
		β	0.0526	0.0358	0.7125	0.0027	0.0044	0.2698	0.0500	0.0336	0.6925
	150	α	−0.0379	0.0404	0.7742	−0.0125	0.0034	0.2284	−0.0357	0.0378	0.7542
		θ	−0.0759	0.1310	1.3882	−0.0046	0.0083	0.3779	0.0721	0.1231	1.3682
		μ	0.0410	0.0250	0.5991	0.0028	0.0024	0.1989	0.0389	0.0231	0.5691
		β	0.0149	0.0182	0.5262	0.0030	0.0021	0.1907	0.0142	0.0163	0.5062

Table 3. Estimation methods under complete sampling for Case III.

$\theta = 0.5,\ \mu = 3,\ \beta = 0.7$										
α	n	Param.	MLE			Bayesian			MPS		
			Bias	MSE	L.CI	Bias	MSE	L.CI	Bias	MSE	L.CI
0.3	40	α	−0.1708	0.4946	1.3784	−0.0100	0.0229	0.2966	−0.1597	0.4601	1.3297
		θ	−0.0176	0.1758	0.8218	−0.0242	0.0306	0.3429	0.1095	0.1582	0.7796
		μ	0.3071	1.8624	2.6747	−0.0070	0.0258	0.3149	0.2485	1.7041	2.5587
		β	0.0536	0.0591	0.4764	0.0084	0.0054	0.1440	−0.0178	0.0537	0.4542
	80	α	−0.1550	0.3842	1.2149	−0.0022	0.0122	0.2165	−0.1478	0.3591	1.1744
		θ	−0.0123	0.1450	0.7464	−0.0217	0.0190	0.2702	0.0909	0.1305	0.7080
		μ	0.2874	1.3435	2.2718	0.0025	0.0168	0.2540	0.2433	1.2625	2.2023
		β	0.0233	0.0381	0.3826	0.0076	0.0032	0.1109	−0.0259	0.0347	0.3651
	150	α	−0.1593	0.3548	1.1675	−0.0057	0.0106	0.2018	−0.1445	0.3241	1.1158
		θ	−0.0065	0.1280	0.7012	−0.0164	0.0167	0.2533	0.0818	0.1146	0.6635
		μ	0.2841	1.2420	2.1842	−0.0005	0.0142	0.2336	0.2319	1.1481	2.1000
		β	0.0183	0.0342	0.3625	0.0070	0.0027	0.1019	−0.0246	0.0308	0.3440
0.5	40	α	−0.1483	0.3709	1.1938	−0.0196	0.0202	0.2786	−0.1375	0.3437	1.1490
		θ	−0.0580	0.2056	0.8887	−0.0247	0.0296	0.3372	0.0966	0.1850	0.8431
		μ	0.3527	2.1314	2.8611	−0.0059	0.0260	0.3161	0.2762	1.9085	2.7081
		β	0.0515	0.0538	0.4546	0.0099	0.0050	0.1386	−0.0183	0.0471	0.4253
	80	α	−0.1393	0.2986	1.0710	−0.0095	0.0116	0.2111	−0.1329	0.2803	1.0377
		θ	−0.0864	0.1682	0.8038	−0.0171	0.0166	0.2525	0.0575	0.1514	0.7626
		μ	0.3209	1.5149	2.4123	0.0008	0.0169	0.2549	0.2534	1.3806	2.3031
		β	0.0245	0.0368	0.3760	0.0067	0.0033	0.1127	−0.0272	0.0327	0.3544
	150	α	−0.1421	0.2033	0.8838	−0.0043	0.0050	0.1386	−0.1349	0.1952	0.8658
		θ	−0.0829	0.1087	0.6463	−0.0108	0.0078	0.1731	0.0283	0.0978	0.6129
		μ	0.3291	0.9183	1.8784	−0.0008	0.0083	0.1786	0.2763	0.8533	1.8107
		β	−0.0096	0.0208	0.2826	0.0064	0.0014	0.0733	−0.0380	0.0187	0.2680
0.8	40	α	−0.1095	0.1716	0.8120	−0.0360	0.0087	0.1829	−0.0992	0.1597	0.7833
		θ	−0.0865	0.2986	1.0710	−0.0229	0.0235	0.3005	0.1057	0.2721	1.0224
		μ	0.5922	2.8509	3.3092	−0.0015	0.0220	0.2907	0.4652	2.5381	3.1224
		β	0.0323	0.0434	0.4084	0.0060	0.0060	0.1518	−0.0399	0.0386	0.3853
	80	α	−0.1307	0.1498	0.7585	−0.0270	0.0062	0.1544	−0.1226	0.1385	0.7294
		θ	−0.0420	0.2391	0.9584	−0.0126	0.0177	0.2607	0.1158	0.2154	0.9098
		μ	0.6438	2.5060	3.1025	0.0010	0.0165	0.2518	0.4931	2.2419	2.9351
		β	0.0065	0.0385	0.3846	0.0040	0.0043	0.1285	−0.0514	0.0343	0.3631
	150	α	−0.1429	0.1263	0.6966	−0.0093	0.0018	0.0832	−0.1351	0.1141	0.6621
		θ	0.0275	0.2074	0.8926	−0.0076	0.0061	0.1531	0.2021	0.1865	0.8465
		μ	0.5339	1.1855	2.1343	0.0021	0.0065	0.1580	0.4496	1.0676	2.0251
		β	−0.0331	0.0211	0.2847	0.0015	0.0015	0.0759	−0.0521	0.0190	0.2702

Table 4. Estimation methods under complete sampling for Case IV.

$\theta = 2,\ \mu = 3,\ \beta = 2$										
α	n	Param.	MLE			Bayesian			MPS		
			Bias	MSE	L.CI	Bias	MSE	L.CI	Bias	MSE	L.CI
0.3	40	α	−0.1484	0.4326	1.2890	−0.0181	0.0161	0.2487	−0.1368	0.4012	1.2414
		θ	−0.1770	0.2950	1.0645	−0.0119	0.0347	0.3651	0.0400	0.2652	1.0093
		μ	0.1424	0.5780	1.4901	−0.0068	0.0235	0.3004	0.1286	0.5132	1.4037
		β	0.0592	0.2571	0.9937	0.0138	0.0232	0.2985	−0.0692	0.2296	0.9391
	80	α	−0.0890	0.2459	0.9718	−0.0088	0.0104	0.1999	−0.0821	0.2268	0.9334
		θ	−0.1109	0.1465	0.7502	−0.0059	0.0192	0.2716	0.0319	0.1312	0.7100
		μ	0.0874	0.3579	1.1725	−0.0052	0.0147	0.2377	0.0816	0.3184	1.1060
		β	0.0264	0.1601	0.7841	−0.0036	0.0146	0.2368	−0.0745	0.1438	0.7433
	150	α	−0.0550	0.1201	0.6793	−0.0055	0.0054	0.1440	−0.0502	0.1085	0.6457
		θ	−0.0614	0.0999	0.6195	−0.0055	0.0121	0.2155	0.0258	0.0899	0.5876
		μ	0.0571	0.2030	0.8830	0.0015	0.0080	0.1753	0.0503	0.1795	0.8303
		β	0.0084	0.0925	0.5961	0.0030	0.0077	0.1720	−0.0566	0.0832	0.5654
0.5	40	α	−0.1353	0.3008	1.0750	−0.0175	0.0110	0.2056	−0.1247	0.2745	1.0270
		θ	−0.2507	0.3642	1.1829	−0.0148	0.0311	0.3456	0.0102	0.3278	1.1223
		μ	0.2299	0.6935	1.6323	−0.0053	0.0264	0.3185	0.2054	0.6232	1.5473
		β	−0.0117	0.1869	0.8475	−0.0027	0.0214	0.2867	−0.1321	0.1678	0.8030
	80	α	−0.0428	0.1283	0.7022	−0.0150	0.0078	0.1731	−0.0420	0.1161	0.6679
		θ	−0.1765	0.2521	0.9842	−0.0086	0.0198	0.2758	0.0279	0.2269	0.9336
		μ	0.0853	0.3797	1.2078	−0.0064	0.0161	0.2487	0.0816	0.3517	1.1623
		β	0.0407	0.1305	0.7080	−0.0054	0.0148	0.2384	−0.0483	0.1172	0.6711
	150	α	−0.0240	0.0547	0.4584	−0.0053	0.0034	0.1143	−0.0234	0.0509	0.4422
		θ	−0.1259	0.1564	0.7751	−0.0010	0.0106	0.2018	0.0297	0.1408	0.7355
		μ	0.0548	0.1740	0.8175	0.0002	0.0087	0.1828	0.0458	0.1633	0.7920
		β	0.0044	0.0606	0.4825	−0.0011	0.0078	0.1731	−0.0420	0.0545	0.4578
0.8	40	α	−0.0922	0.0740	0.5331	−0.0250	0.0038	0.1208	−0.0628	0.0687	0.5137
		θ	−0.1701	0.3228	1.1137	−0.0005	0.0306	0.3429	0.0154	0.2905	1.0565
		μ	0.4793	1.0771	2.0343	0.0065	0.0301	0.3401	0.4185	0.9694	1.9299
		β	−0.0056	0.1045	0.6335	−0.0156	0.0216	0.2881	−0.0958	0.0941	0.6012
	80	α	−0.0595	0.0394	0.3890	−0.0148	0.0021	0.0898	−0.0374	0.0355	0.3693
		θ	−0.1310	0.2109	0.9002	0.0063	0.0187	0.2681	0.0218	0.1898	0.8539
		μ	0.3220	0.6489	1.5789	−0.0051	0.0169	0.2548	0.3226	0.5840	1.4980
		β	−0.0023	0.0637	0.4947	−0.0045	0.0148	0.2385	−0.0599	0.0573	0.4693
	150	α	−0.0316	0.0130	0.2235	−0.0091	0.0010	0.0620	−0.0148	0.0117	0.2120
		θ	−0.0578	0.1153	0.6657	−0.0040	0.0109	0.2046	0.0461	0.1038	0.6314
		μ	0.1841	0.2869	1.0500	0.0053	0.0104	0.1998	0.1706	0.2582	0.9960
		β	−0.0003	0.0289	0.3332	−0.0035	0.0072	0.1315	−0.0357	0.0260	0.3163

Table 5. Bayesian estimates under censored sampling for Cases V–VII.

				Case V			Case VI			Case VII		
				$\alpha=0.5,\ \theta=2,\ \mu=3,\ \beta=2$			$\alpha=0.5,\ \theta=0.5,\ \mu=3,\ \beta=2$			$\alpha=0.5,\ \theta=0.5,\ \mu=0.5,\ \beta=2$		
				Bayesian			Bayesian			Bayesian		
n	T	d	Param.	Bias	MSE	L.CI	Bias	MSE	L.CI	Bias	MSE	L.CI
40	0.15	28	α	−0.0149	0.0106	0.3872	−0.0050	0.0158	0.4816	−0.0067	0.0178	0.5211
			θ	−0.0119	0.0192	0.5197	−0.0197	0.0210	0.5487	−0.0141	0.0232	0.5842
			μ	−0.0060	0.0195	0.5478	−0.0053	0.0197	0.5252	−0.0035	0.0031	0.2177
			β	−0.0084	0.0178	0.5291	−0.0029	0.0174	0.5136	−0.0089	0.0180	0.5072
		35	α	−0.0155	0.0096	0.3646	−0.0124	0.0160	0.4668	−0.0014	0.0164	0.4951
			θ	−0.0012	0.0172	0.5115	−0.0165	0.0198	0.5308	−0.0133	0.0186	0.5319
			μ	−0.0040	0.0168	0.5055	−0.0023	0.0166	0.4930	−0.0051	0.0029	0.2066
			β	0.0024	0.0164	0.4882	−0.0027	0.0174	0.5039	−0.0026	0.0161	0.4822
	0.35	28	α	−0.0140	0.0091	0.3641	−0.0148	0.0152	0.4628	−0.0063	0.0173	0.5035
			θ	−0.0067	0.0192	0.5054	−0.0213	0.0210	0.5604	−0.0086	0.0220	0.5646
			μ	0.0011	0.0167	0.4997	−0.0020	0.0186	0.5330	−0.0017	0.0023	0.1918
			β	0.0035	0.0176	0.5313	−0.0029	0.0178	0.5040	−0.0057	0.0172	0.5129
		35	α	−0.0177	0.0087	0.3492	−0.0098	0.0145	0.4612	−0.0071	0.0134	0.4404
			θ	−0.0035	0.0171	0.5101	−0.0175	0.0175	0.5177	−0.0110	0.0176	0.5078
			μ	−0.0014	0.0166	0.4984	0.0023	0.0154	0.4777	−0.0002	0.0015	0.1585
			β	−0.0030	0.0152	0.4846	−0.0034	0.0167	0.5084	−0.0093	0.0143	0.4659
150	0.15	100	α	−0.0128	0.0061	0.2919	−0.0204	0.0130	0.4268	−0.0071	0.0160	0.4773
			θ	−0.0060	0.0190	0.5522	−0.0207	0.0214	0.5792	−0.0163	0.0182	0.5241
			μ	−0.0059	0.0189	0.5378	−0.0023	0.0180	0.5261	−0.0049	0.0013	0.1427
			β	0.0023	0.0140	0.4716	−0.0036	0.0146	0.4720	−0.0088	0.0145	0.4852
		130	α	−0.0125	0.0052	0.2728	−0.0139	0.0113	0.4003	−0.0013	0.0123	0.4134
			θ	−0.0066	0.0169	0.5046	−0.0154	0.0195	0.5559	−0.0114	0.0165	0.4959
			μ	0.0028	0.0157	0.4853	0.0000	0.0162	0.4840	−0.0043	0.0012	0.1340
			β	−0.0017	0.0127	0.4464	−0.0023	0.0151	0.4675	−0.0023	0.0122	0.4332
	0.35	100	α	−0.0152	0.0056	0.2779	−0.0167	0.0113	0.4087	−0.0050	0.0145	0.4523
			θ	−0.0025	0.0188	0.5438	−0.0175	0.0197	0.5415	−0.0256	0.0198	0.5396
			μ	0.0009	0.0162	0.4793	0.0030	0.0151	0.4788	−0.0021	0.0011	0.1294
			β	−0.0121	0.0140	0.4634	−0.0059	0.0139	0.4539	−0.0008	0.0142	0.4519
		130	α	−0.0084	0.0046	0.2645	−0.0155	0.0110	0.4034	−0.0038	0.0121	0.4042
			θ	−0.0007	0.0169	0.4953	−0.0175	0.0185	0.5244	−0.0171	0.0156	0.4860
			μ	−0.0008	0.0146	0.4761	0.0036	0.0114	0.4093	−0.0019	0.0007	0.1024
			β	−0.0035	0.0113	0.4193	−0.0045	0.0125	0.4422	0.0010	0.0100	0.3978

once take either minimum. The margin is not marginal. Averaged over all combinations, the Bayesian MSE is 16.8%, 12.4%, 6.1% and 8.3% of the corresponding MLE value in Cases I–IV respectively, so that the reduction in MSE is at worst a factor of six and at best a factor of sixteen. The same advantage is visible in the average absolute bias, which is 0.005–0.010 for the Bayesian estimator against 0.060–0.156 for the MLE and 0.041–0.148 for the MPS estimator, although on this criterion the Bayesian procedure is not universal: it yields the smallest absolute bias in 32–34 of the 36 combinations per case, with the remaining few shared between the MLE and the MPS estimator. The Bayesian intervals are also markedly shorter, never exceeding an average length of about 0.6 in the cases studied, whereas the corresponding MLE intervals are frequently two to four times as long. The superiority of the Bayesian approach is most pronounced for the shape parameter α and for the parameter μ in the cases where μ is large. In Case III, for example, the MLE of μ has an average MSE of 1.728 under complete sampling, against 0.017 for the Bayesian estimator, and the corresponding MPS figure of 1.567 offers essentially no improvement over the MLE. This behaviour is a familiar consequence of the strong asymmetry of the conditional likelihood for μ when the true value is well away from the origin: the Newton–Raphson iterations are drawn towards the boundary of the parameter space, and the resulting estimates carry a heavy positive bias that inflates both the MSE and the interval length. The gamma prior damps this drift, and the MCMC sampler explores the skewed posterior region far more faithfully than a quadratic approximation around the likelihood maximum can. The MLE and the MPS estimators behave almost identically throughout, differing typically in the third decimal place, which suggests that the two procedures, although derived from different objective functions, are tracking the same likelihood surface in these configurations.

The expected qualitative effects are confirmed quantitatively. Increasing the sample size reduces the Bayesian MSE in each case by a factor of roughly three between $n = 40$ and $n = 150$ from 0.0133 to 0.0043 in Case I, from 0.0157 to 0.0050 in Case II, from 0.0188 to 0.0069 in Case III and from 0.0228 to 0.0078 in Case IV while the bias and the interval length shrink in step. The ordering of the cases is equally stable: Case I is systematically the easiest to estimate and Case IV the hardest, which reflects the increasing distance of μ from its prior centre and the corresponding widening of the posterior. Increasing α from 0.3 to 0.8 has a smaller and less uniform effect, generally reducing the MSE for α and β while leaving the θ and μ components dominated by the sample size.

Table 5 shows that the Bayesian estimator retains its advantage when the sample is hybrid censored. Biases remain small in absolute terms across the whole design, never exceeding 0.0177 in Case V, 0.0213 in Case VI and 0.0256 in Case VII, and the interval lengths are of the same order as those obtained under complete sampling. The comparative magnitudes of the three censored cases mirror the complete-sample ordering: Case V, in which the parameter configuration is closest to the prior centre, yields the smallest maximum MSE (0.0195) and the shortest maximum interval (0.5522), while Case VII, in which both θ and μ are small, produces the largest of each (0.0232 and 0.5842). Two features of the censored design deserve particular comment. First, increasing the number of observed failures r improves precision at a fixed sample size and censoring time, and the improvement is remarkably consistent: the mean Bayesian MSE falls in all twelve comparisons, by between 5.5% and 13.0% when r rises from 28 to 35 at $n = 40$, and by between 7.3% and 22.6% when it rises from 100 to 130 at $n = 150$. Second, relaxing the censoring time from $T = 0.15$ to $T = 0.35$ also improves the estimates in every one of the twelve comparisons, though by a smaller margin that ranges from 0.8% to 14.0%. Taken together, these two effects indicate that the information lost to censoring is recovered more efficiently by observing a larger proportion of failures than by extending the observation window, at least over the range of T considered here. The effect of the sample size itself is more muted under censoring than under complete sampling the mean Bayesian MSE falls by only about 15% between $n = 40$ and $n = 150$ within a fixed T and r ratio because at $n = 150$ the censoring time binds before the sample is exhausted and the effective information gain is correspondingly smaller. The parameter μ in Case VII is an instructive exception to the general pattern. Its Bayesian MSE is roughly an order of magnitude smaller than those of the remaining parameters (between 0.0007 and 0.0031 against 0.010–0.023 elsewhere), and its interval length is correspondingly short, contracting from 0.2177 at $n = 40$, $r = 28$ to 0.1024 at $n = 150$, $r = 130$. With $\mu = 0.5$ and $\alpha = \theta = 0.5$, the prior is centred almost exactly on the true value and the likelihood is close to symmetric over the region the sampler visits, so the posterior is both tight and nearly Gaussian. This configuration is therefore the most favourable in the whole censored design and serves as a useful benchmark for the behaviour of the estimator when the prior is well calibrated. Conversely, the θ component is the least well determined in

the censored cases, with MSEs of 0.015–0.023 that are broadly flat across n, r and T; under hybrid censoring the termination time carries comparatively little information about θ once the number of failures is held fixed.

The overall conclusion is unambiguous. Under both complete and hybrid censored sampling, and across every parameter configuration, sample size and censoring scheme examined, the Bayesian estimator with gamma priors under the SE loss function outperforms both the maximum likelihood and the maximum product of spacings estimators, in some settings by more than an order of magnitude in MSE and by a factor of several in interval length. The two classical procedures remain close to each other throughout, which suggests that the gain reported here is attributable to the prior information and the posterior sampling rather than to any particular property of the objective function being maximised. Since the hyperparameters were calibrated so that the prior mean and variance match those of the corresponding estimators, this is a comparison that deliberately favours the Bayesian approach, and the margin should be read accordingly; a study in which the priors are mis-specified would be the natural next step, and would indicate how much of the advantage survives when the prior is no longer anchored to the truth.

6. Goodness-of-Fit–Based Empirical Data Analysis

In this section, two real datasets are analyzed and discussed in order to demonstrate the flexibility of the new generator. The Akaike information criterion (AIC), the consistent Akaike information criterion (CAIC), the Hannan–Quinn information criterion (HQIC), the Kolmogorov–Smirnov (KS) statistic with its associated P-value, the Anderson–Darling statistic (A^*), and the Cramér–von Mises statistic (W^*) are used as statistical criteria for judging the fit in this study.

6.1. Dataset I

The dataset consists of survival times, measured in days, for 72 guinea pigs infected with virulent tubercle bacilli, as reported by [5]. Nonparametric plots are presented in Figure 4 to examine the shape and distributional characteristics of the data.

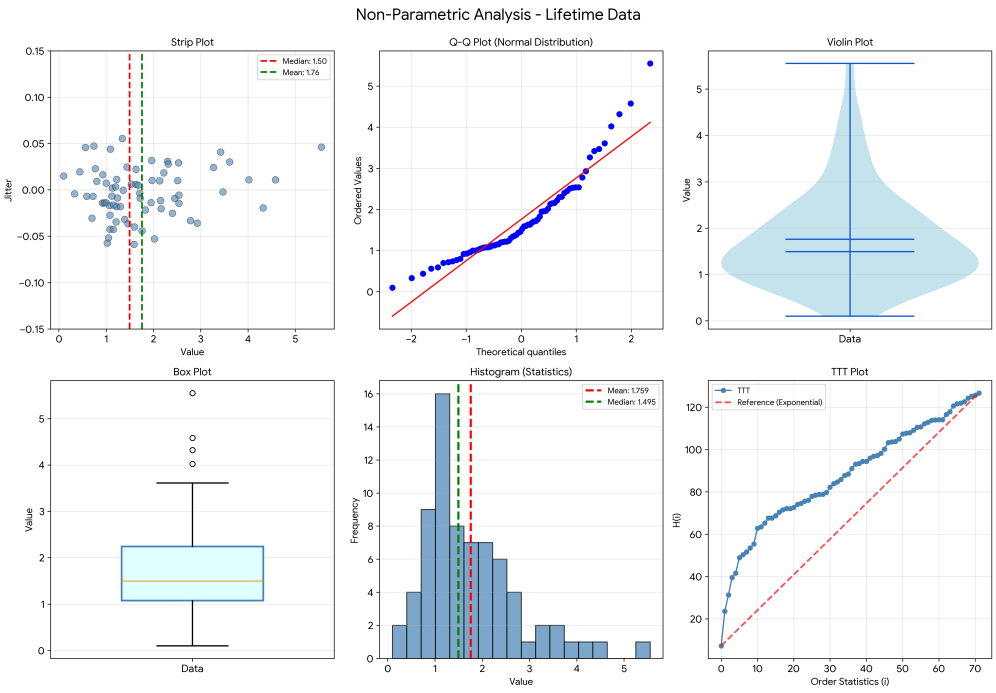


Figure 4. Nonparametric plots for Dataset I.

The dataset exhibited a positively skewed distribution, with values ranging from 0.10 to 5.55. Most observations were concentrated between 0.7 and 2.5, indicating a predominance of relatively low values. The mean (≈ 1.77) was higher than the median (≈ 1.50), suggesting a right-skewed distribution influenced by a few higher observations. The presence of relatively high values (4.58 and 5.55) indicates variability within the dataset. Overall, the results suggest a non-symmetrical distribution, with most observations clustered at lower values and a few elevated values contributing to the overall variability. Therefore, the dataset can be analyzed using the WG-NB family of distributions. The WENB distribution is a special case of this family, obtained by considering the exponential distribution as the baseline model G. The WENB distribution is compared with some continuous rival models, namely the exponential (E), Weibull exponential (WE), exponential exponential (EE), Rayleigh exponential (RE) and exponentiated Weibull exponential (EWE). Tables 6 and 7 provide the MLEs and metrics of goodness of fit. The advantage of the WENB model is shown when compared with all examined models. Based on the goodness-of-fit criteria, the WENB model provides the best fit to the observed data among all competing distributions considered.

Table 6. Estimates for Dataset I.

	μ		α		β		θ	
Model↓Parameter⟶	MLE	SE	MLE	SE	MLE	SE	MLE	SE
E	0.5445	0.0642	-	-	-	-	-	-
RE	0.0017	0.0031	68341.6	2.43×10^{5}	-	-	-	-
EE	0.2744	0.0747	1.2966	0.5525	-	-	-	-
WE	0.0198	0.0145	146.412	582.82	1.5694	0.1258	-	-
EWE	0.0304		32.429		1.0623		2.2778	
WENB	0.1211	0.0284	0.9466	0.01885	2.1646	0.2145	1.4628	0.6458

Table 7. Goodness-of-fit criteria for Dataset I.

Model	$-L$	AIC	$CAIC$	$HQIC$	KS	$P\text{-}value$	A^*	W^*
E	115.7726	233.5451	233.6023	234.4515	0.26902	5.956×10^{-5}	5.9039	1.4445
RE	107.581	219.163	219.337	220.975	0.14056	0.11622	2.3224	0.4522
EE	110.134	224.269	224.442	226.081	0.18585	0.01384	2.8029	0.4808
WE	104.295	214.589	214.942	217.309	0.11574	0.28966	1.1378	0.1884
EWE	102.929	213.858	214.455	217.483	0.10205	0.44147	0.7174	0.1070
WENB	93.427	194.854	195.451	198.479	0.08526	0.67188	0.4366	0.0580

The graphical assessment of the goodness-of-fit performance of the competing distributions is presented in Figure 5. These plots provide a visual evaluation of how closely the theoretical cumulative probabilities agree with the corresponding empirical probabilities. This finding indicates that the WENB model effectively captures the underlying distributional characteristics of the survival times of guinea pigs infected with virulent tubercle bacilli. Furthermore, this graphical evidence supports the results obtained from the numerical goodness-of-fit criteria, confirming the suitability and flexibility of the proposed distribution for modelling the observed survival data. To investigate the behaviour of the likelihood function and assess the stability of the maximum likelihood estimates (MLEs), Figures 6 and 7 illustrate the profile log-likelihood functions corresponding to the unknown parameters of the WENB distribution as well as the contour plots. Each profile is obtained by varying one parameter while keeping the remaining parameters fixed at their estimated values. The resulting curves exhibit well-defined peaks, indicating the existence of identifiable maxima of the log-likelihood function. The presence of these peaks provides graphical evidence that the numerical estimation procedure successfully identifies parameter values associated with high likelihood values. Moreover, the smoothness and curvature of the log-likelihood profiles provide insight into the sensitivity of the likelihood function to changes in individual parameters. These results support the stability of the estimated parameters and suggest that the WENB model is appropriately specified for the observed dataset. However, the graphical appearance of a single maximum does not necessarily establish the global uniqueness of

the MLEs. In addition to MLE, the MPS and Bayesian estimation methods are employed to estimate the unknown parameters of the WENB distribution using the complete dataset. The corresponding parameter estimates are reported in Table 8.

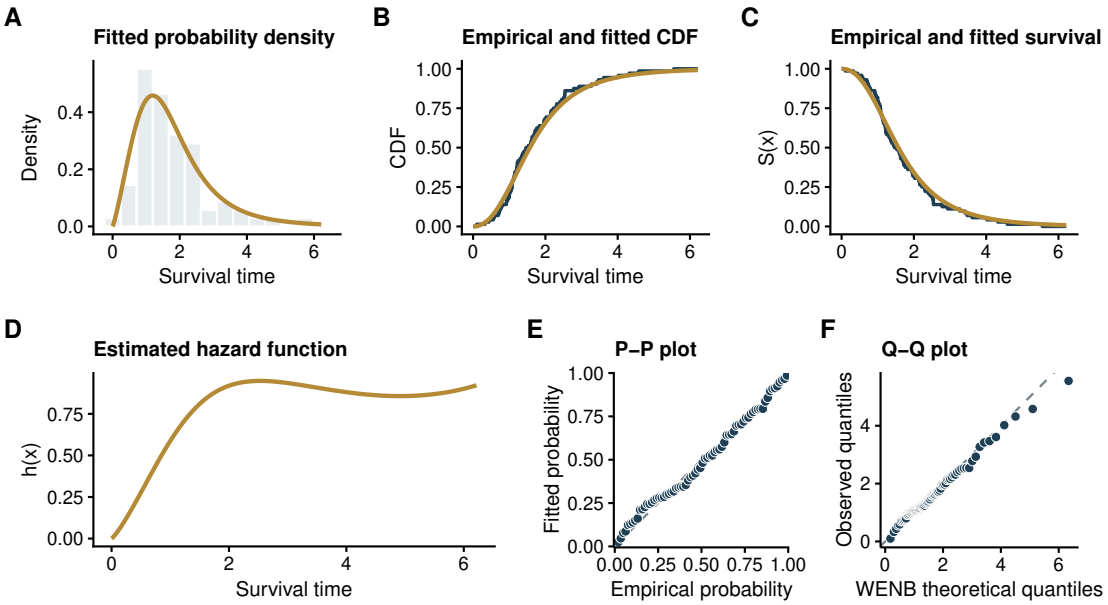


Figure 5. Fitted plots for Dataset I.

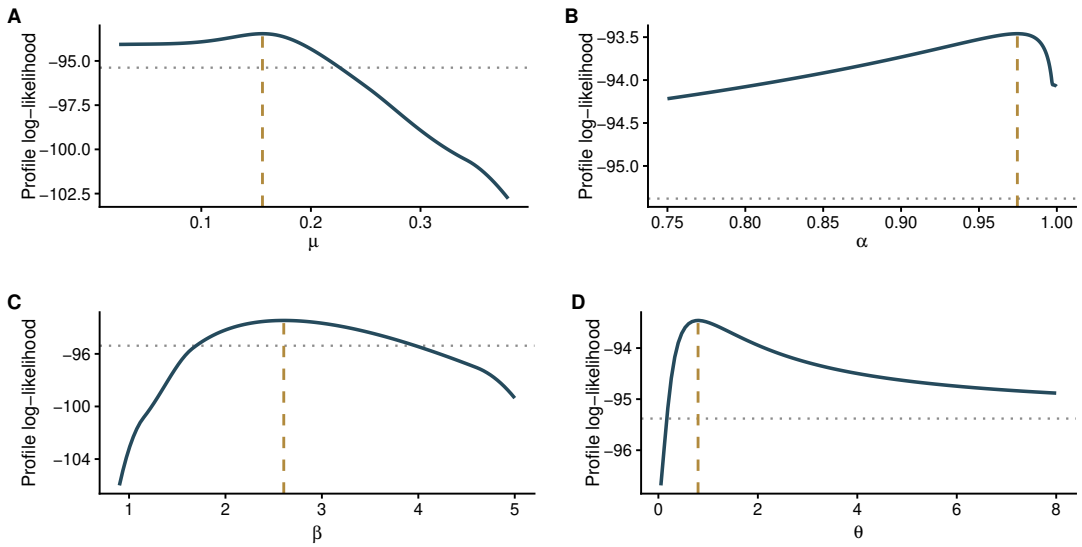


Figure 6. Profile log-likelihood corresponding to Dataset I.

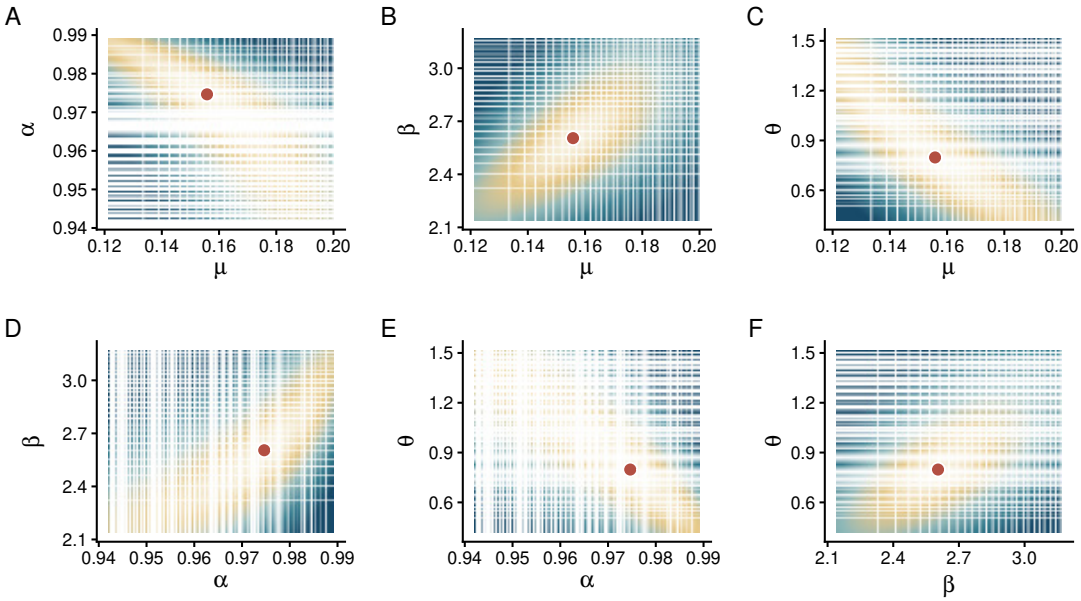


Figure 7. Contour plots corresponding to Dataset I.

Table 8. MPS and Bayesian estimators for Dataset I.

		estimates	SE	Lower	Upper
MPS	α	0.974748	0.047654	0.881346	0.999000
	θ	1.705659	0.970693	0.196900	3.608217
	μ	0.073193	0.063501	0.015127	0.197655
	β	2.058857	0.30948	1.452276	2.665438
Bayesian	α	0.809756	0.071343	0.643086	0.990198
	θ	2.428828	0.922297	0.486015	3.131621
	μ	0.143101	0.04055	0.06248	0.225431
	β	1.929668	0.265523	1.420739	2.441967

The MPS approach provides an alternative estimation procedure based on maximizing the geometric mean of the spacings between consecutive fitted cumulative probabilities. In contrast, the Bayesian approach incorporates prior information and observed data through the posterior distribution to obtain parameter estimates. Comparing the estimates obtained from these methods allows an assessment of their numerical agreement and provides additional insight into the reliability of parameter estimation for the proposed distribution. Furthermore, Figures 8 and 9 present the MCMC trace plots, convergence reference lines, and marginal posterior probability density functions (PDFs) for the unknown parameters of the WENB distribution.

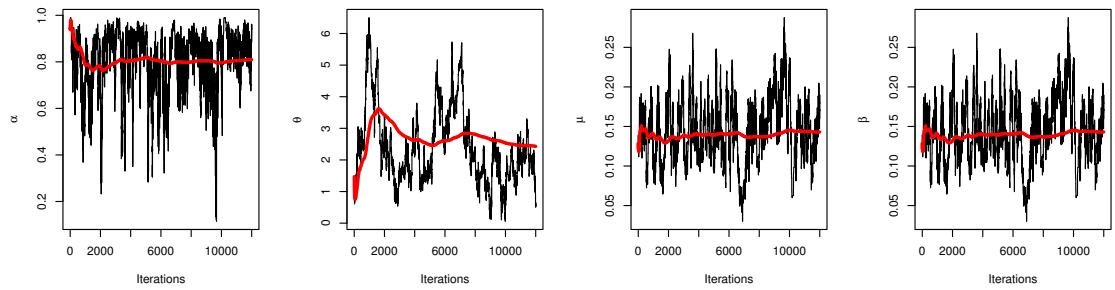


Figure 8. Trace plot of MCMC results for Dataset I.

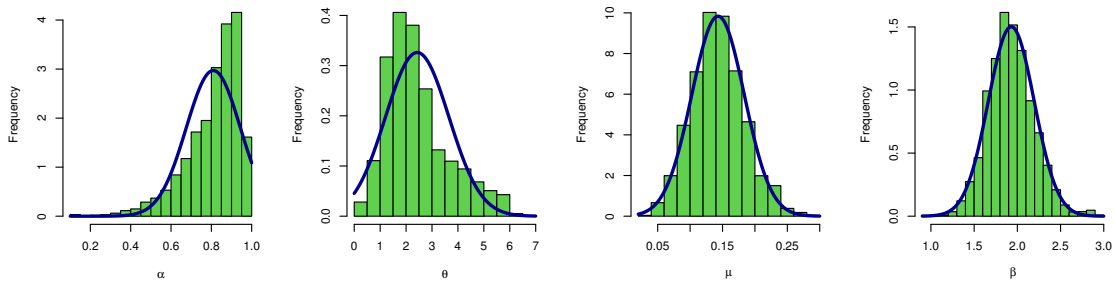


Figure 9. The histogram plot of MCMC results for Dataset I.

These graphical diagnostics are used to evaluate the sampling behavior of the MCMC algorithm, examine the convergence characteristics of the generated chains, and investigate the shapes of the marginal posterior distributions. The trace plots illustrate the variation of the simulated parameter values across successive MCMC iterations, providing information about the stability and mixing behavior of the Markov chains. In particular, chains that fluctuate around relatively stable levels without systematic trends provide encouraging evidence of convergence toward the target posterior distributions. The marginal posterior PDFs provide further information about the location, spread, and shape of the posterior distributions, allowing an assessment of parameter uncertainty. Well-defined posterior density curves indicate regions of relatively high posterior probability and facilitate the interpretation of Bayesian parameter estimates. Taken together, these graphical diagnostics provide useful evidence regarding the performance of the Bayesian estimation procedure, although formal convergence diagnostics, such as effective sample sizes and potential scale reduction factors, are also recommended to confirm satisfactory MCMC convergence.

6.2. Dataset II

The second dataset consists of 100 observations on the breaking stress of carbon fibers (in GPa), originally reported by Nichols and Padgett [23]. Nonparametric plots for dataset II are shown in Figure 10.

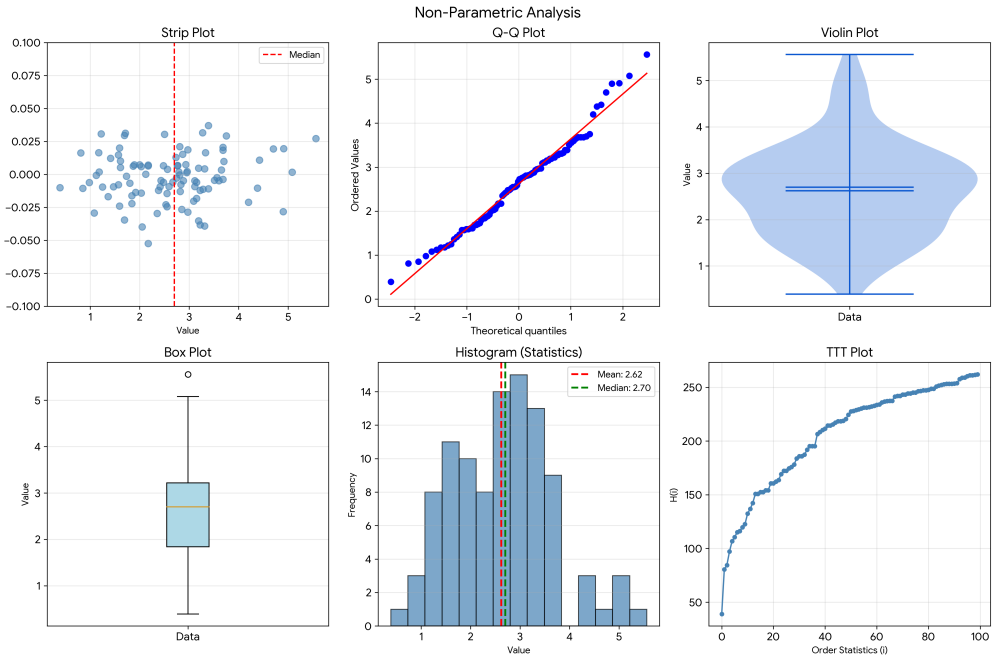


Figure 10. Nonparametric plots for Dataset II.

The data exhibit moderate variability, with values ranging approximately from 0.39 GPa to 5.56 GPa, indicating the presence of both relatively weak and relatively strong fibres within the sample. A preliminary exploratory analysis suggests a right-skewed, positively supported distribution, with most observations concentrated around lower to moderate stress levels and a few larger values acting as potential high-strength outliers. This distributional shape is typical of lifetime and strength data and supports the use of flexible parametric models commonly applied in reliability analysis. Consequently, the dataset provides a suitable test bed for assessing the adequacy and flexibility of the proposed WG-NB model in comparison with existing competing distributions. The WFNB distribution is compared with various continuous rival models, including Kumaraswamy Fréchet (KF), exponentiated Fréchet (EF), beta Fréchet (BF), gamma extended Fréchet (GEF), transmuted Marshall–Olkin Fréchet (TMOF), transmuted Fréchet (TF), Marshall–Olkin Fréchet (MOF), and Fréchet distributions. Tables 9 and 10 present the MLEs and corresponding goodness-of-fit measures. Indeed, the WFNB model demonstrates superiority when juxtaposed against all examined models.

Table 9. Estimates for Dataset II.

	a		b		θ		β		α	
Model↓Parameter⟶	MLE	SE	MLE	SE	MLE	SE	MLE	SE	MLE	SE
Fr	1.8705	0.112	1.7766	0.113	-	-	-	-	-	-
TF	1.9315	0.097	1.7435	0.076	-	-	-	-	-	-
MOF	2.3066	0.498	1.5796	0.16	0.5988	0.3091	-	-	-	-
TMOF	0.6496	0.068	3.3313	0.206	101.923	47.625	0.2936	0.27	-	-
GEF	1.3692	2.017	0.4776	0.133	27.6452	14.136	17.4581	14.818	-	-
EF	69.1489	57.349	0.5019	0.08	145.3275	122.924	-	-	-	-
KF	2.0556	0.071	0.4654	0.00701	6.2815	0.063	224.18	0.164	-	-
BF	1.6097	2.498	0.4046	0.108	22.0143	21.432	29.7617	17.479	-	-
WFNB	1.4339		0.5215		1.0874		3.74741		0.00679	

Table 10. Goodness-of-fit criteria for Dataset II.

Model	$-L$	AIC	$CAIC$	$HQIC$	KS	$P-value$	A^*	W^*
Fr	172.15	348.3	348.4	350.4	0.1722	0.0053	5.4918	0.9220
TF	172.25	350.5	350.7	353.6	0.1737	0.0048	5.4631	0.9142
MOF	172.65	351.3	351.6	354.5	0.1813	0.0028	5.3599	0.8834
TMOF	151.00	310.0	310.4	314.2	0.1212	0.1060	1.9543	0.3426
GEF	152.00	312.0	312.4	316.2	0.1354	0.0511	2.1613	0.4083
EF	144.85	295.7	296.0	298.9	0.1021	0.2480	0.9201	0.1901
KF	144.55	297.1	297.5	301.3	0.0991	0.2802	0.8517	0.1756
BF	151.55	311.1	311.6	315.4	0.1343	0.0543	2.0923	0.3969
WFNB	141.531	293.063	293.701	298.334	0.0751	0.6253	0.4736	0.0883

Figure 11 illustrates the estimated plots for Dataset II. The graphical findings demonstrate the effectiveness and flexibility of the proposed WFNB distribution in modelling the observed dataset. Its ability to closely approximate the empirical CDF suggests that it offers a more accurate representation of the underlying probability structure than the TMOF, GEF, EF, KF, and BF distributions. Additionally, the profile log-likelihood analysis provides a useful assessment of the reliability of the WFNB parameter estimates. These findings support the WFNB model as a promising alternative for analyzing datasets with complex distributional characteristics. However, its overall superiority should also be confirmed through quantitative goodness-of-fit measures, information criteria, and appropriate statistical comparisons.

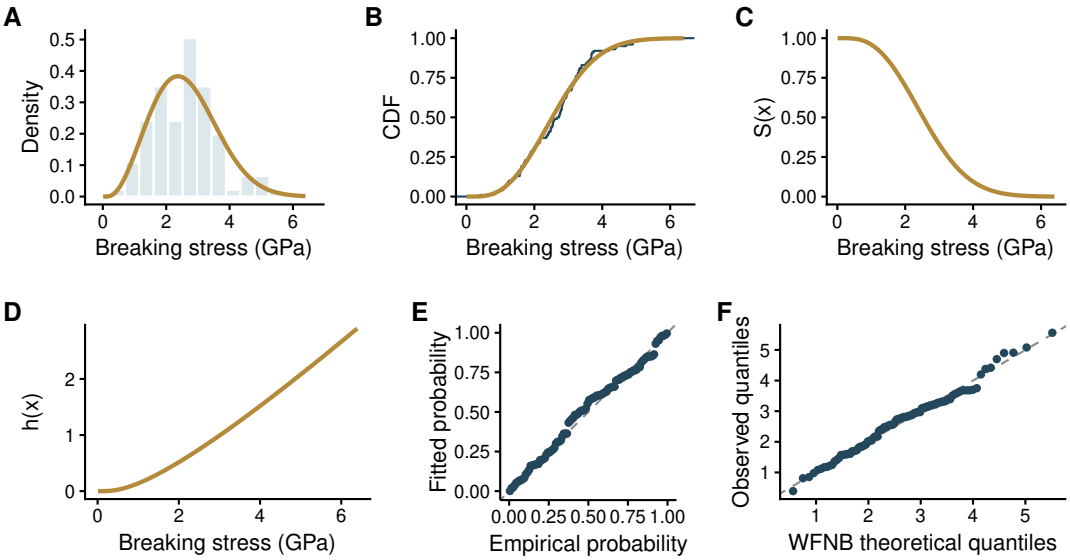


Figure 11. Estimated plots for Dataset II.

In addition to the MLE approach, the MPS and Bayesian estimation methods are used to estimate the unknown parameters of the WFNB distribution based on the entire Dataset II. The results show that the MPS and Bayesian estimates are very close to their MLE counterparts, showing the consistency and dependability of the proposed estimators in multiple inferential frameworks. Further, the unimodality of the profile log-likelihood functions for each parameter is noted confirming the existence of unique global maxima and supporting the stability of the likelihood based estimate technique. The MCMC diagnostics (trace plots, convergence reference lines and marginal

posterior PDFs) provide strong evidence that the chains have converged and mixed well for all unknown parameters of the WFNB model, from a Bayesian perspective, thus confirming the reliability of the posterior summaries.

7. Conclusion

In this paper, a novel and flexible extension of the W-G family was introduced, termed the WG-NB distribution, which addressed several limitations of existing lifetime and reliability models. This new distribution combined the W-G framework with the G-NB mixing scheme, resulting in a highly adaptable model capable of capturing a wide range of hazard rate shapes, including monotonic, unimodal, and bathtub-like patterns, making it suitable for analyzing complex lifetime data. The theoretical properties of the distribution, such as moments, entropy measures, and other key characteristics, were systematically derived. Both classical and Bayesian inference procedures were developed and validated through extensive simulation studies. Empirical applications on two real datasets demonstrated the model's superior fitting performance and practical utility. Overall, it was concluded that the WG-NB distribution served as a versatile, robust, and efficient tool for survival analysis and reliability engineering, offering notable improvements over existing models. Future research directions included potential extensions to multivariate contexts, incorporation of covariates, and advanced computational methods to enhance its applicability and effectiveness.

Acknowledgments

The authors extend their appreciation to Prince Sattam bin Abdulaziz University for funding this research work through the project number (PSAU/2025/01/35309).

Data Availability

The dataset is included within the paper.

Conflict of Interest

The authors have disclosed no conflicts of interest.

REFERENCES

[1] Abdelaziz, M. A., Cordeiro, G. M., Nofal, Z. M., & Afify, A. Z. (2025). A comprehensive survey of Weibull-based families. *Journal of Statistical Models and Methods, 1*(1), 98–118.

[2] Afify, A. Z., Nassar, M., & Cordeiro, G. M. (2026). Unit odd-G classes of distributions: Mathematical foundations, regression modeling, and applications to economic indices. *Statistical Methods & Applications, 35*(1), 45–72.

[3] Alzaatreh, A., Famoye, F., & Lee, C. (2024). Recent developments in T-X family of distributions: Extended Weibull generators and applications. *Journal of Statistical Theory and Practice, 18*(2), 34–52.

[4] Badr, M. M., Elbatal, I., Jamal, F., Chesneau, C., & Elgarhy, M. (2020). The transmuted odd Fréchet-G family of distributions: Theory and applications. *Mathematics, 8*(5), 958–978.

[5] Bjerkedal, T. (1960). Acquisition of resistance in guinea pigs infected with tubercle bacilli. *American Journal of Hygiene, 72*(2), 130–148.

[6] Bourguignon, M., Silva, R. B., & Cordeiro, G. M. (2014). The Weibull-G family of probability distributions. *Journal of Data Science, 12*(1), 53–68.

[7] Chen, M. H., & Shao, Q. M. (1999). Monte Carlo estimation of Bayesian credible and HPD intervals. *Journal of Computational and Graphical Statistics, 8*(1), 69–92.

[8] Cheng, R. C. H., & Amin, N. A. K. (1983). Estimating parameters in continuous univariate distributions with a shifted origin. *Journal of the Royal Statistical Society: Series B (Methodological), 45*(3), 394–403.

[9] Cordeiro, G. M., & de Castro, M. (2011). A new family of generalized distributions. *Journal of Statistical Computation and Simulation, 81*(7), 883–898.

[10] Cordeiro, G. M., Chesneau, C., & Yousof, H. M. (2024). The power odd Weibull-G family: Mathematical formulations, inference, and engineering applications. *Journal of Computational and Applied Mathematics, 438*, 115521.

[11] Eliwa, M. S., El-Morshedy, M., & Shahen, H. (2023). A discrete analogue of odd Lomax generator for extreme and zero-inflated count data. *Filomat, 37*(18), 6063–6080.

[12] Eliwa, M. S., Shahen, H. S., El-Dawoody, M., & El-Morshedy, M. (2025). A flexible bivariate skewed odd-G family of distributions for various hazard rate profiles in dispersed trends. *AIMS Mathematics, 10*(10), 23025–23066.

[13] Eliwa, M. S., Tahir, M. H., Hussain, M. A., Almohaimeed, B., & Al-Bossly, A. (2023). Univariate probability-G classes for scattered samples under different forms of hazard. *Mathematics, 11*(13), 2929.

[14] El-Morshedy, M., Eliwa, M. S., & Tyagi, A. (2022). A discrete analogue of odd Weibull-G family of distributions. *Journal of Applied Statistics, 49*(11), 2928–2952.

[15] El-Morshedy, M., & Eliwa, M. S. (2024). A bivariate probability generator for the odd generalized exponential model. *Filomat, 38*(3), 1109–1133.

[16] Eugene, N., Lee, C., & Famoye, F. (2002). Beta-normal distribution and its applications. *Communications in Statistics—Theory and Methods, 31*(4), 497–512.

[17] Glänzel, W. (1987). A characterization theorem based on truncated moments and its application to some distribution families. In *Mathematical statistics and probability theory (Bad Tatzmannsdorf, 1986)* (Vol. B, pp. 75–84). D. Reidel.

[18] Glänzel, W. (1990). Some consequences of a characterization theorem based on truncated moments. *Statistics: A Journal of Theoretical and Applied Statistics, 21*(4), 613–618.

[19] Hajebi, M., Rezaei, S., & Nadarajah, S. (2013). An exponential negative binomial distribution. *REVSTAT—Statistical Journal, 11*(2), 191–210.

[20] Marshall, A. W., & Olkin, I. (1997). A new method for adding a parameter to a family of distributions with application to the exponential and Weibull families. *Biometrika, 84*(3), 641–652.

[21] Moakofi, T., Oluyede, B., & Warahena-Liyanage, G. (2026). The new Marshall-Olkin type II exponentiated half logistic-Gompertz-G family of distributions: Properties and applications. *Computational Journal of Mathematical and Statistical Sciences, 5*(2), 553–589.

[22] Nassar, M., Afify, A. Z., & Kumar, D. (2024). A unit-extended Weibull distribution: Properties, estimation methods, and modeling proportional data. *Communications in Statistics—Simulation and Computation, 53*(4), 1890–1912.

[23] Nichols, M. D., & Padgett, W. J. (2006). A bootstrap control chart for Weibull percentiles. *Quality and Reliability Engineering International, 22*, 141–151.

[24] Ortega, E., Cordeiro, G. M., & Kattan, M. (2012). The negative binomial-beta Weibull regression model to predict cure of prostate cancer. *Journal of Applied Statistics, 39*(6), 1191–1210.

[25] Osi, A. A., Abdalla, G. S. S., Singh, N. S. S., & Suleiman, A. A. (2025). Advancing lifetime data modeling via the Marshall-Olkin cosine Topp-Leone distribution family. *Computational Journal of Mathematical and Statistical Sciences, 4*(2), 476–499.

[26] Percontini, A., Cordeiro, G. M., & Bourguignon, M. (2013). The G-negative binomial family: General properties and applications. *Advances and Applications in Statistics, 35*(2), 127–160.

[27] Ramos, M. W. A., Percontini, A., Cordeiro, G. M., & da Silva, R. V. (2015). The Burr XII negative binomial distribution with applications to lifetime data. *International Journal of Statistics and Probability, 4*(1), 109.

[28] Rodrigues, C., Cordeiro, G. M., Demétrio, C., & Ortega, E. (2011). The Weibull negative binomial distribution. *Advances and Applications in Statistics, 22*(1), 25–55.

[29] Tahir, M. H., Alizadeh, M., & Mansoor, M. (2025). Trigonometric extensions of odd-G distributions with applications to censored biomedical data. *Reliability Engineering & System Safety, 243*, 109871.

[30] Tahir, M. H., Zubair, M., Cordeiro, G. M., Alzaatreh, A., & Mansoor, M. (2017). The Weibull-power Cauchy distribution: Model, properties and applications. *Hacettepe Journal of Mathematics and Statistics, 46*(4), 767–789.

[31] Yousof, H. M., Ali, M. M., & Ibrahim, M. (2025). Bayesian and classical estimation of the extended odd Weibull parameters under progressive type-II hybrid censoring. *Quality and Reliability Engineering International, 41*(1), 115–134.

[32] Yousof, H. M., Ali, M. M., & Khosa, S. K. (2026). Bayesian inference and maximum product of spacings estimation for generalized odd-G models under adaptive progressive censoring. *Quality and Reliability Engineering International, 42*(1), 89–108.

[33] Zamani, H., & Ismail, N. (2010). Negative binomial-Lindley distribution and its application. *Journal of Mathematics and Statistics, 6*(1), 4–9.

[34] Zografos, K., & Balakrishnan, N. (2009). On families of beta- and generalized gamma-generated distributions and associated inference. *Statistical Methodology, 6*(4), 344–362.